R-04-45

Applications of hydrogeological modelling methodology using NAMMU and CONNECTFLOW

Task 1, 2, 3 and 4

Björn Gylling, Niko Marsic
Kemakta Konsult AB

Lee Hartley, David Holton
Serco Assurance

November 2004

Svensk Kärnbränslehantering AB
Swedish Nuclear Fuel
and Waste Management Co
Box 5864
SE-102 40 Stockholm Sweden
Tel 08-459 84 00
+46 8 459 84 00
Fax 08-661 57 19
+46 8 661 57 19

ISSN 1402-3091
SKB Rapport R-04-45

Applications of hydrogeological modelling methodology using NAMMU and CONNECTFLOW

Task 1, 2, 3 and 4

Björn Gylling, Niko Marsic
Kemakta Konsult AB

Lee Hartley, David Holton
Serco Assurance

November 2004

Abstract

It is planned to store spent nuclear fuel at depth in crystalline rock in Sweden. Site investigations are carried out to confirm if the suggested sites are appropriate. Modelling of groundwater flow and transport may be used to aid the site investigation and is also an important part of the safety assessment of a site. A good design of the repository will enhance the safety. To support the site investigation phase and the design of underground repositories four tasks have been performed. These tasks are all related to the CONNECTFLOW groundwater flow modelling concept. CONNECTFLOW is a suite of software that includes:

- the continuum porous medium (CPM) concept as implemented in NAMMU,
- the discrete fracture network (DFN) concept as implemented in NAPSAC,
- the ability to nest these two representations into a single combined model.

As an integrated suite of hydrogeological modelling tools CONNECTFLOW offers several benefits:

- the ability to nest different scales of the model from the canister-scale to the regional-scale to resolve detailed flow behaviour around the waste packages in the context of the overall hydrogeological situation at a site,
- nesting is flexible as embedded fine-scale CPM regions can be nested within coarser CPM models, multiple DFN regions can be nested inside CPM models, and CPM models can be nested within DFN models,
- nesting of regions is precise in that the system is solved in a single step with equations at the interface between nested regions that ensure both continuity of pressure and conservation of mass flux between the regions. This ensures a flux-balance between the two-scales, and hence offers greater consistency than two-step nesting or only implementing pressure continuity,
- the ability to upscale DFN models to obtain the equivalent CPM properties on a variety of scales ensures that the modeller can move between DFN and SC concepts easily in a self-consistent way.

The aim of the current tasks is to demonstrate and test the CONNECTFLOW concept, show the workflow from data to model, and create generic though realistic models that can be adapted for later studies.

Models for Task 1, 2, 3 and 4 have been set up. In all cases nested models have been created using CONNECTFLOW. Task 1 and 2 consider the case of a repository-scale DFN model nested within an embedded CPM model that includes both the site-scale and regional-scales. Task 1 demonstrates how such models can be constructed. Task 2 shows what results can be obtained using such a model by applying the model to Beberg and comparing the results for canister flux and transport statistics with results from pure CPM models as used in SR 97. Several realisations of the model were performed and analysed to obtain statistics of repository performance measures such as groundwater travel time and flux at starting positions. The results show good consistency in the mean values when compared to SR 97, but the variance is increased in the new nested model. This is to be expected since a DFN model offers much greater resolution in local-scale variability since it represents individual fractures on a few metres scale rather than the CPM approach where flows are

effectively averaged out over a larger volume (e.g. 35 m cuboid elements). Task 2 gave also an opportunity to test the recently developed method to calculate F-quotients directly in CONNECTFLOW.

For Task 3 the converse arrangement of nesting was used where a rather complex CPM model was nested within a DFN model. The CPM model represents a tunnel system with an access tunnel, six deposition tunnels and 162 deposition holes. A generic DFN model serves as a framework and makes it possible to study fracture and repository intersections. The goal is to obtain detailed near-field flow rates and possibility to address design issues.

In Task 4, the CONNECTFLOW concept is used to calculate more realistic input to a near-field model since it models explicitly the flow in the fracture system around the canisters together with the exchange of flow between the natural fracture system and the backfilled tunnels and deposition holes. The CONNECTFLOW model described in Task 3 is used for this purpose as it includes a more appropriate level of detail required to quantify issues of flow around canister locations and in the adjacent engineered structures.

To overcome the limitations in previous statistical package built on Statistica, a new package is built based on Matlab. Matlab provides larger arrays, more flexibility and includes better options for programming. In this project the new statistical package denoted @STAT is tested and used to illustrate some of the results.

Sammanfattning

Det är planerat att djupförvara använt kärnbränsle i Sverige. Platsundersökningar görs för att ge underlag för utredningar om lämplighet av föreslagna platser. Modellering av grundvattenflöde och transport av däri lösta ämnen kan användas för att ge stöd åt platsundersökningarna och därmed utgöra ett viktigt redskap i säkerhetsanalysen av en plats. Säkerhetsnivån förstärks naturligtvis av en god förvarskonstruktion. För att stödja platsundersökningarna och utredningar angående olika förvarsalternativ har vi utfört fyra olika modelleringsuppgifter. I samtliga fyra modelleringsuppgifter har vi använt grundvattenmodelleringskonceptet CONNECTFLOW. CONNECTFLOW är ett program-paket som innehåller:

- det modellkoncept som är implementerat i NAMMU och som beskriver ett kontinuerligt poröst medium (CPM),
- det diskreta nätverkskoncept (DFN) som även är implementerat i NAPSAC och
- möjligheten att nästla dessa två representationssätt i en och samma modell.

Detta integrerade paket av hydrogeologiska modellredskap som CONNECTFLOW utgör erbjuder flera fördelar:

- Möjligheten att nästla olika modellskalor t ex från kapselskala till regional skala. Detta möjliggör att man kan beskriva ett detaljerat flödesmönster på förvarsnivå samtidigt som den övergripande hydrogeologiska situationen beskrivs.
- Nästlingstekniken är flexibel så till vida att man kan nästla en finskalig CPM-domän inuti en grövre CPM-modell. Man kan även lägga in multipla DFN-områden inuti en CPM-modell. Det är också möjligt att lägga in en CPM-modell inuti en DFN-modell.
- Det nästlade modellkonceptet innehåller ekvationer både för att beskriva ett kontinuerligt tryckfält och för att bevara massflödet över gränssnittet mellan de kopplade domänerna. I och med att dessa ekvationer löses i ett steg erhålls en mycket god överensstämmelse av tryck och flöde över gränssnittet mellan de nästlade modellområdena. Jämfört med att utföra nästlingen i ett tvåstegsförfarande eller att bara införa tryckkontinuitet erhålls en bättre överensstämmelse mellan modelldomänerna.
- Genom att använda en inbyggd uppskalningsteknik i DFN-konceptet är det möjligt att beräkna motsvarande CPM-egenskaper. Detta gör det möjligt för modellören att enkelt byta koncept från DFN till CPM eller tvärtom och samtidigt behålla en storskalig överensstämmelse mellan modellkoncepten.

Syftet med modellövningarna i denna rapport är att demonstrera och testa CONNECTFLOW-konceptet, visa arbetsflödet från data till modell, och att sätta upp generiska men realistiska modeller som kan komma till användning i kommande studier.

Modeller för modelluppgifterna 1, 2, 3 och 4 har satts upp och i samtliga fall har modellerna skapats i CONNECTFLOW. Uppgift 1 och 2 berör fall där en DFN-modell i förvarsskala är nästlad i en CPM-modell som innefattar både platsskala och regional skala. Uppgift 1 beskriver hur denna typ av modell sätts upp. I uppgift 2 används denna modell för att modellera Beberg och för att beräkna specifikt flöde vid kapselpositioner och transport-statistik. Dessa resultat jämförs med motsvarande resultat från den typ av CPM-modell som användes i SR 97. Ett flertal realiseringar med den uppsatta modellen beräknades för att erhålla statistik för några mätetal av förvarsfunktionen såsom advektiv gångtid och specifikt flöde vid startpositioner. Resultaten visar god överensstämmelse med de

medelvärden som togs fram i SR 97, men variansen är större i den här nya nästlade modellen. Detta är inte överraskande i och med att det använda DFN-konceptet erbjuder en högre upplösning och variabilitet i den lokala skalan då konceptet kan representera meterstora sprickor i stället för i fallet med ett CPM-koncept där flöde och transport är medelvärdat över större volymer, t ex 35 m kubiska element. Modelluppgift 2 gav dessutom ett tillfälle att testa den relativt nya metoden att beräkna F-termen direkt i CONNECTFLOW.

I modelluppgift 3 har det motsatta förfarandet använts vid nästlingen av modellkoncept då en relativt komplicerad CPM-modell var nästlad inuti en DFN-modell. Här representerar CPM-modellen ett tunnelsystem med en accesstunnel, sex depositionstunnlar och 162 depositionshål. En generisk DFN-modell används som ramverk och gör det möjligt att studera skärningen mellan sprickor och förvaret. Målet är här att erhålla en mer detaljerad bild av flödet i närzonen och att kunna adressera konstruktionsfrågor.

I modelluppgift 4 har CONNECTFLOW använts för att beräkna mer realistiska indata till en närzonsmodell. Detta möjliggörs genom att man kan modellera flödet i spricksystemet runt förvaret samtidigt som utbytet av flöde mellan det naturliga spricksystemet och de återfyllda tunnlarna och depositionshålen erhålls. Den CONNECTFLOW-modell som sattes upp i modelluppgift 3 användes här eftersom den erbjuder en tillräcklig detaljeringsgrad för att kunna studera flöden runt kapselpositioner och förvarstunnlar.

För att överkomma de begränsningar som finns i det statistikprogram som är baserat på Statistica, har ett nytt program utvecklats i Matlab. Matlab erbjuder större datafält, högre flexibilitet och en bättre programmeringsmiljö. I detta projekt har det nya statistikpaketet, som har namngivits till @STAT, testats och använts för att illustrera en del av resultaten.

Contents

1 Introduction

It is planned to store spent nuclear fuel at depth in crystalline rock in Sweden. Site investigations are going to be carried out to confirm if the suggested sites are appropriate. Modelling of groundwater flow and transport may be used to aid the site investigation and is also an important part of the safety assessment of a site. A good design of the repository will enhance the safety. To support the site investigation phase and the design of underground repositories, four tasks have been initiated. These tasks are described in Table 1-1. The tasks all relate to the CONNECTFLOW groundwater flow modelling concept. CONNECTFLOW is a suite of software that includes:

- the CPM concept as implemented in NAMMU /Cliffe et al. 1998/,
- the DFN concept as implemented in NAPSAC /Hartley et al. 2002/,
- the ability to nest these two representations into a single combined model /Hartley and Holton, 2003/.

A glossary of the used abbreviations is given in Table 1-2.

This project is a co-operation between Kemakta Konsult AB and Serco Assurance, and funded by SKB (The Swedish Nuclear Fuel and Waste Management Company). Some of the tasks are coupled to the activities in the international group iCONNECT. The members in the group are users of CONNECTFLOW.

As mentioned, the model concepts used in this project are CPM and DFN. The software package CONNECTFLOW contains both NAMMU (CPM) and NAPSAC (DFN). Both NAMMU and NAPSAC use a finite-element discretisation technique. NAMMU has been successfully applied in previous SKB studies, both in the regional-scale and the local-scale. For example, in SR 97 /Walker et al. 2001/, NAMMU was used to obtain

Table 1-1. Definition of Tasks 1 to 4.

Task	Description	Purpose
1. CONNECTFLOW site-scale model	Nest a repository scale DFN model within a continuum model of Beberg.	Demonstration and verification of CONNECTFLOW concept. Provide a test-case for iCONNECT: DFN nested within CPM/SC.
2. Simulate canister location process	Simulate process of canister location to avoid high flow regions in stochastic and heterogeneous models. Use NAMMU and Task 1 models.	Automate the process of choosing particle start position in stochastic DFN and SC models to avoid fracture zones and regions of high flow.
3. CONNECTFLOW repository-scale model	Nest a detailed CPM model of deposition holes and tunnels in a DFN mode.	Demonstration and verification of CONNECTFLOW concept. Provide a test-case for iCONNECT: CPM nested within DFN.
4. Near-field/ geosphere integration	Interface detailed canister-scale hydrogeological models to near-field (COMP23) input. Using either DFN models (Task1) or CONNECTFLOW (Task3).	Provide more realistic models of near-field by using input parameters derived from discrete fracture models, and models with an explicit representation of tunnels and barriers.

Table 1-2. Glossary of the used abbreviations.

CONNECTFLOW	A suite of software including NAMMU and NAPSAC that allows nested models of the two concepts to be combined
DFN	Discrete Fracture Network
SC	Stochastic Continuum
CPM	Continuum Porous Medium

a general understanding of the Beberg /Hartley et al. 1998/ and Ceberg /Boghammar et al. 1997/ sites and to supply local-scale models with boundary conditions /Gylling et al. 1999; Walker and Gylling, 1999/. Some of the capabilities of NAPSAC were demonstrated by /Holton and Milický, 1997/. In Section 1.1 more information on the modelling software may be found.

1.1 Modelling concepts

1.1.1 CONNECTFLOW

CONNECTFLOW (CONtinuum and NEtwork Contaminant Transport and FLOW) is an advanced software package for modelling groundwater flow and transport in porous and fractured media /Serco Assurance, 2004/. It is based on the NAMMU and NAPSAC software, and provides all of the functionality of NAMMU and NAPSAC. In addition, it enables combined models to be built consisting of NAMMU (porous media) and NAPSAC (fractured media) sub-models. This allows the most appropriate models to be used and the flexibility to change between concepts easily. It incorporates full 3D grid generation and post-processing capabilities, and uses one of the most robust and reliable solvers available.

1.1.2 NAMMU

NAMMU (Numerical Assessment Method for modelling Migration Underground) is a finite-element software package for modelling groundwater flow and transport in porous media. It incorporates full 3D grid generation and post-processing capabilities, and uses one of the most robust and reliable solvers available. It can be used to model:

- Groundwater flow in saturated and unsaturated conditions,
- Anisotropic permeability (arbitrary orientation),
- Multiple species contaminant transport, including the effects of advection, dispersion and sorption,
- Coupled groundwater flow and salt transport with density dependent on concentration,
- Coupled groundwater flow and heat transport,
- 3D, 2D cross-sectional and 2D areal flows, and
- Sensitivity to model parameters, using the adjoint sensitivity method.

The finite-element method used by NAMMU is ideally suited for accurate modelling of complex geological systems. Grid generation facilities are available for modelling complex geologies incorporating rock sections, fractures, boreholes and engineered features. Local mesh refinement is straightforward. These features enable the user to generate models quickly, making full use of all available data.

1.1.3 NAPSAC

NAPSAC is a finite-element software package for modelling groundwater flow and transport in fractured rock. A discrete fracture network approach is used to model groundwater flow and the transport of contaminants through the fractured rock. NAPSAC incorporates full 3D model generation and post-processing capabilities. It has the following capabilities:

- Fractures can be defined deterministically or stochastically with specified distributions of lengths, strikes, dips and transmissivities.
- Transmissivity can vary over individual fractures.
- Calculation of equivalent continuum properties.
- Flow to or from boreholes and tunnels intersecting the fracture network can be modelled.
- Contaminant transport can be modelled using particle tracking.
- Steady-state and time-dependent calculations can be made, and
- 2D and 3D calculations can be made.
- Groundwater flow in saturated and unsaturated conditions.

NAPSAC uses efficient numerical algorithms, which enable very large fracture networks (containing hundreds of thousands of fractures) to be modelled. The finite-element method is used to model flows through individual fractures, allowing detailed calculations of the flow to be made in the vicinity of boreholes and on fractures with varying transmissivity.

1.2 Scope of work

This project involves preparations for the coming studies e.g. within the iCONNECT Club. In a way this is a pre-project to initiate projects related to the modelling tool CONNECTFLOW and an opportunity for training in the use of this concept for Kemakta staff.

Task 1 has the aim of illustrating how nested repository-scale, local-scale and regional-scale models can be constructed using CONNECTFLOW. This is described in Section 2.

Based on the Task 1 model, Task 2 is designed to show how these models can be applied to site-assessment studies and what benefits it offers over a pure porous media or indirect nesting approaches. Section 3 deals with Task 2.

Task 3 is described in Section 4. This task involves a more detailed study of the near-field flow by a generic application of CONNECTFLOW. A canister-scale CPM sub-region is nested within a DFN model of the repository-scale fractures.

Task 4 uses this canister-scale model to consider the differences in deriving input for a near-field model based on more detailed models when compared to earlier methods that used larger scale CPM models. Task 4 is reported in Section 5.

To overcome the limitations in previous statistical package built on Statistica, a new package is built based on Matlab. Matlab provides larger arrays, more flexibility and includes better options for programming. In this project the new statistical package denoted @STAT is tested and used to illustrate some of the results. The technical documentation on @STAT will be reported separately.

2 CONNECTFLOW site-scale model

A part of the work related to the iCONNECT Club is intended to create a series of test-case models to illustrate the capabilities of the software. These test cases will also be used as a basis for verifying the applicability of the concept to realistic models and as tutorials for training purposes.

Task 1 consists of setting up a CONNECTFLOW application by nesting a repository-scale DFN sub-region (say 1 km by 1 km by 50 m) within a continuum porous medium model of the site-scale and regional-scale. The resulting model may be used in later tasks, e.g. in the iCONNECT club, to address some more specific issues in later tasks.

For illustrative purposes an existing NAMMU model of Beberg was combined with DFN data from Aberg /Dershowitz et al. 1999/, obtained from the AMP project /Selroos et al. 2002/. Figure 2-1 shows an example of such a model using synthetic DFN data.

Some objectives of this task are:

- To study the feasibility of calculating flows on such nested models.
- To determine the appropriate size of model as a function of fracture concept.
- To be able to represent fracture zones consistently.
- To calculate pathline statistics.
- To analyse the statistical convergence of stochastic models.

The project also gives an opportunity to Kemakta staff for an introduction to the use of CONNECTFLOW. Therefore, this task is coupled to some more general training in CONNECTFLOW.

A further aim of the task will be to consider the workflow in creating such relatively complex nested models and whether this might need to be adapted in general or to SKB's particular needs.

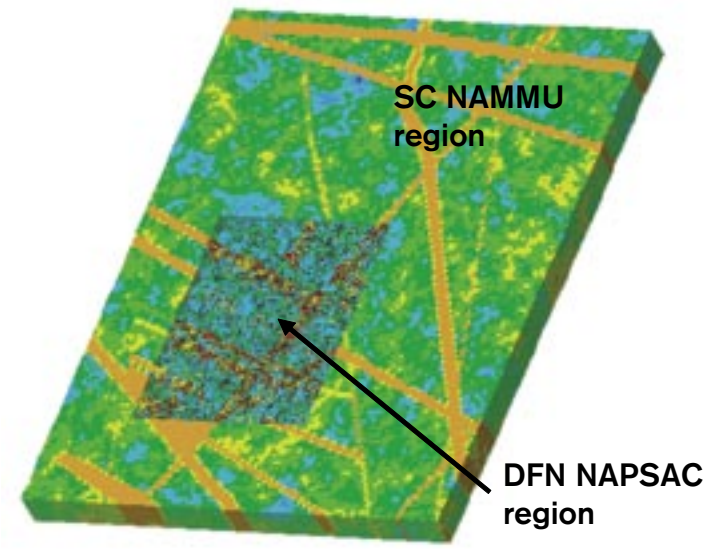

Figure 2-1. *Example of nesting repository-scale DFN model in a SC site-scale model.*

2.1 Modelling approach

The model developed in Task 1 consists of three parts: a DFN region to model a 50 m layer within the northern rock block to represent part of the hypothetical repository, a detailed CPM local-scale model surrounding the repository, and finally a large regional-scale CPM model to capture the regional groundwater flow pattern. The structure of these regions can be seen in Figure 2-2 and Figure 2-3.

The CPM regions are based on Beberg data, using the IFZ (Implicit Fracture Zone) method to define fracture zones. The DFN model is set up to cover a section of the northern repository. As input data for the deterministic fracture zones in the DFN, the information from IFZ is used. Aberg data from the Alternative Model Project (AMP) calculations was used to include the fracture statistics for the stochastic fractures.

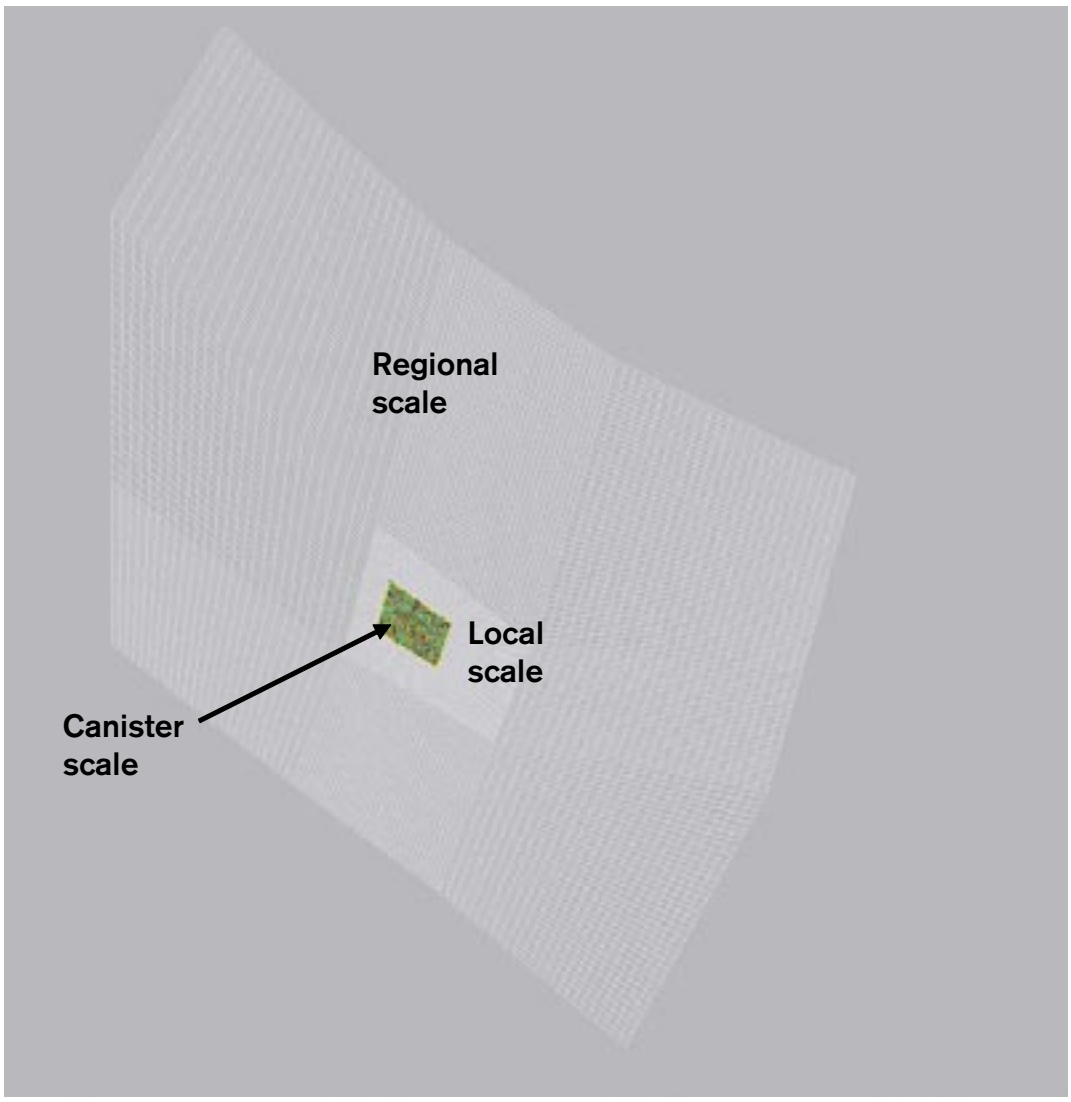

Figure 2-2. *Plan View of the full model with the regional- and local-scale CPM models and the central DFN canister-scale region model.*

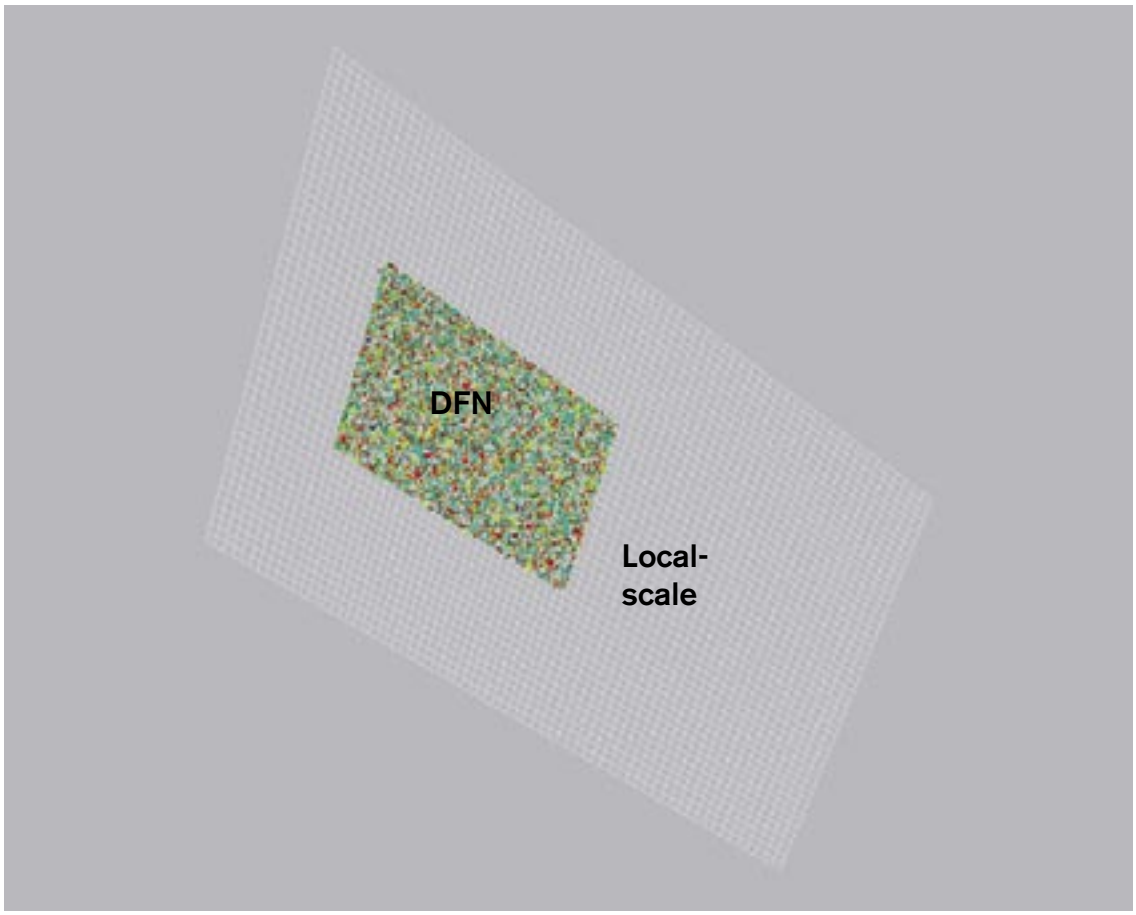

Figure 2-3. *Amplified from Figure 2-2, it shows the grid in the local-scale CPM model and the DFN region nested within. The fractures are coloured by set.*

CONNECTFLOW was run in batch mode since a Graphical User Interface (GUI) is not yet available. However, a GUI is available for NAPSAC and this was used to create the input data for the DFN part of the model. The data input file for CONNECTFLOW is essentially the super-set of data commands for NAMMU and NAPSAC. Hence, the CONNECTFLOW input data file was created by merging the relevant commands for the NAPSAC part into a pre-existing file for a NAMMU model of Beberg. Some minor editing was then made to nest the models. The input language for CONNECTFLOW differs slightly from NAPSAC at the top level of commands so as to distinguish the NAPSAC part. The NAMMU commands are unchanged.

The CONNECTFLOW model was visualised in AVIZIER for CONNECTFLOW to study and verify the set-up. Based on the same information it is not surprising that the agreement in the location of fracture zones across the model interface is good, as can be seen in Figure 2-4.

It can be seen that the location and extension of the DFN part covers most of the northern repository. The resulting CONNECTFLOW model contains about 300,000 CPM finite-elements and about 85,000 fractures. It would be possible to alter the size and shape of the DFN region to cover the whole repository region, but the size of the current model was already utilising the available RAM, about 900 Mb.

2.1.1 Data used and assumptions

The CPM regions are based on Beberg data. The size of the regional model is roughly 10×16×1.5 km. It is divided into five main layers in the vertical direction to define the repository layer and a depth trend of the permeability field. These layers are subdivided into about 100 m thick elements in the regional scale. Horizontally, the grid is divided into approximately 40 patches per layer and then further discretized (using about 10 to 50 divisions per patch in each direction). An embedded grid ("Constraints") method in NAMMU is used to refine the local-scale region by a factor of 2 compared to the regional-scale. The grid created in this way is more refined in the inner local-scale model (35–40 m) than in the outer regional scale model (80–200 m). The total number of CPM elements is approximately 300,000. The permeability variation with depth is defined as piecewise constant in three layers: near surface, above 850 m below sea level (bsl) and below 850 m bsl. Ten different types of rock were used in the CPM models to represent the depth trend in permeability, but also to aid visualisation. The permeability, porosity and specific storage coefficients for each of these rocks are given in Table 2-1.

The IFZ (Implicit Fracture Zone) method is used to define the fracture zones in the CPM region. Based on /Walker et al. 1997/, the permeability is incremented with respect to the base value by a factor of approximately 2.4 in the southern block region (delimited by Zone 14, Zone 13, Zone 3e, Zone 5 and Zone 1b) and by a factor of 5.5 in the northern rock region (delimited by Zone 1b, Zone 12, Zone 14 and Zone 5). The CPM model was created as a SC by calculating the permeability for each element from an exponential variogram for permeability and accounting for the fracture zones by use of IFZ.

The DFN model is set up to cover a section of the northern repository. The size of the DFN model is roughly 1×1×0.05 km. This region is modelled by a single hexahedra. As input data for the deterministic (known) fracture zones the information for IFZ is used. It was translated to NAPSAC format by using one of the available options. The option used is to model the known fracture zones as limited planes divided into triangles using the GOCAD format. The continuity of the fracture zones from the CPM to the DFN regions can be appreciated in Figure 2-4, where the fractures are coloured by transmissivity and the finite-elements by permeability. Figure 2-5 shows the transmissivity of the fractures in the DFN model.

Table 2-1. Permeabilities, porosity and specific storage coefficient for different types of rocks in the CPM models.

Rock name	Geometric mean K_{xx} (m^2)	Geometric mean K_{yy} (m^2)	Geometric mean K_{zz} (m^2)	Geometric standard deviation in Log K	Φ	Specific Storage Coefficient
'NSRFR1'	1.55×10^{-14}	1.55×10^{-14}	1.55×10^{-14}	0.46	10^{-4}	10^{-10}
'BZN2R1'	1.26×10^{-15}	1.26×10^{-15}	1.26×10^{-15}	0.32	10^{-4}	10^{-11}
'BZN2R2'	1.26×10^{-15}	1.26×10^{-15}	1.26×10^{-15}	0.32	10^{-4}	10^{-11}
'BZN2R3'	1.26×10^{-15}	1.26×10^{-15}	1.26×10^{-15}	0.32	10^{-4}	10^{-11}
'BASER1'	5.00×10^{-16}	5.00×10^{-16}	5.00×10^{-16}	0.32	10^{-4}	10^{-11}
'NSRFL1'	6.92×10^{-15}	6.92×10^{-15}	6.92×10^{-15}	0.83	10^{-4}	10^{-10}
'BZN2L1'	5.62×10^{-16}	5.62×10^{-16}	5.62×10^{-16}	0.83	10^{-4}	10^{-11}
'BZN2L2'	5.62×10^{-16}	5.62×10^{-16}	5.62×10^{-16}	0.83	10^{-4}	10^{-11}
'BZN2L3'	5.62×10^{-16}	5.62×10^{-16}	5.62×10^{-16}	0.83	10^{-4}	10^{-11}
'BASEL1'	5.62×10^{-16}	5.62×10^{-16}	5.62×10^{-16}	0.83	10^{-4}	10^{-11}

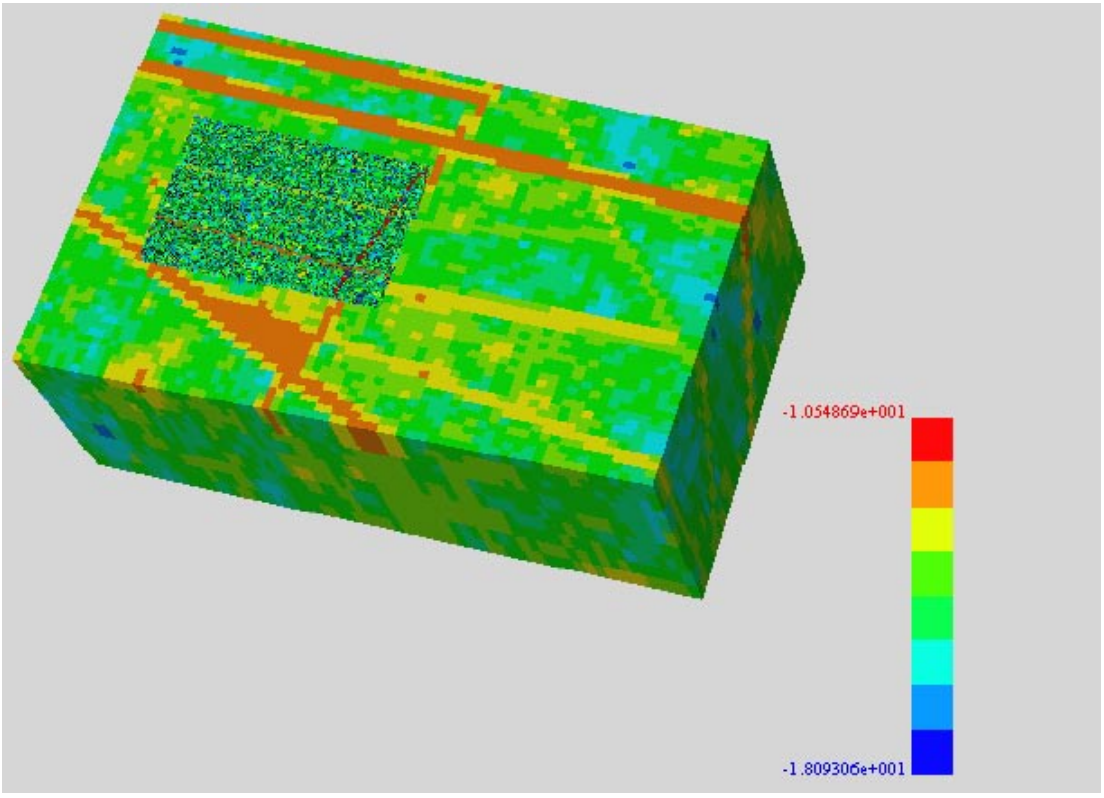

Figure 2-4. *Permeability of CPM elements and transmissivity of fractures. Only the local-scale part of the model is shown. High permeability/transmissivity is coloured red, low values are blue. The correspondence of the fracture zones in the CPM and DFN regions can be observed.*

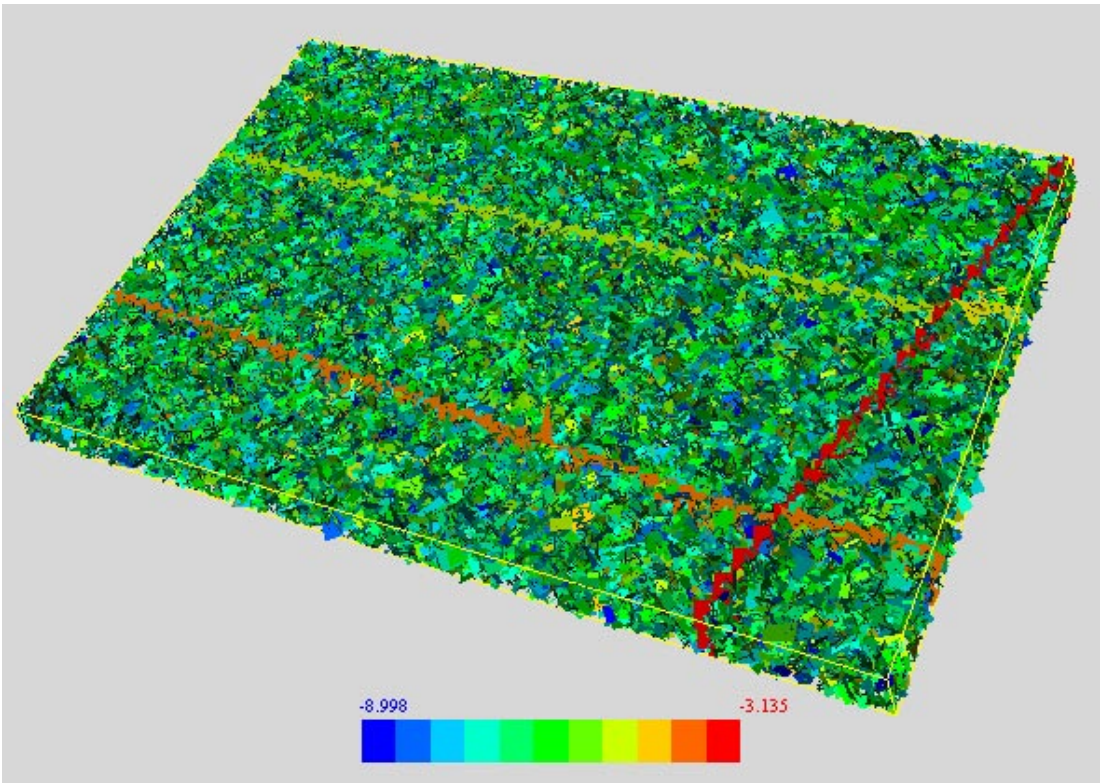

Figure 2-5. *Transmissivity of the random fractures in the DFN region on a logarithmic scale. The red colour signifies high transmissivity, blue means low.*

Aberg data was used to include the fracture statistics for the stochastic features. Here, data from the AMP calculations are used (see Table 2-2, /Dershowitz et al. 1999/. The data include information for two sets. One set is for fractures of the order of 100 m, and the other set is for fractures of the order of 10 m. Each set is then divided into three orientation sub-sets, as is shown in Table 2-3, based on data from /Poteri, 1996/.

The total number of planes in the DFN model is approximately 85,000, with an average surface area per unit volume (P32) of 0.218 m^{-1}. The total number of fracture intersections in the full model is about 200,000.

A boundary condition of the constraints type must be applied in the interface between the regional- and local-scale CPM models in order to make finite-element interpolations of the variables continuous across the interface. The ground surface topography is used for the head boundary condition on the upper surface of the CPM region. No-flow boundary conditions are used for external vertical and lower boundaries.

The boundary condition at the interface between the DFN and CPM models is of two-way coupling type. That is, the pressure in the DFN region is coupled to the pressure in the CPM model and flux is conserved across the interface.

Table 2-2. Data used from the FracMan AMP report by /Dershowitz et al. 1999/.

DFN Parameter	Assumption
Fracture Size Distribution f(R)	Lognormal
(Repository Region)	Mean = 6 m
	Std.Dev = 3 m
	Truncated to 0.2 < R < 20 m
Fracture Transmissivity	Truncated Lognormal
Distribution f(T)	Mean = 9.0e–7 m^2/s
	Std.Dev. = 5.0e–6 m^2/s
	Tmin = 1.0e–09 m^2/s
Conductive Intensity	P_{32} = 0.2 m–1
Conductive Intensity (above T_{min} and R_{min})	P_{32} = 0.038 m–1 (Model Region)
	P_{32} = 0.2 m–1 (Repository Region)
Transport Aperture	$0.5T^{0.5}$

Table 2-3. Used orientation distributions from /Poteri, 1996/.

Set	Dispersion	Strike [o]	Dip [o]	Relative Intensity
1	1.0	309	2	0.35
2	8.9	212	14	0.23
3	18	329	87	0.22

2.2 Results

The coupled CONNECTFLOW model was solved for flow using an iterative preconditioned conjugate gradient algorithm. It takes about 60 minutes to solve the system on a single Dell Pentium 4 1.0GHz processor. The main constraint on the size of model was the available memory (RAM) that was about 950 Mb for Kemakta's current Linux configuration.

The flow across the interface between regions was studied. The flux from one region to the other was $2.67 \cdot 10^{-2}$ m^3/s, or an average flow of about $2 \cdot 10^{-8}$ m/s. The preliminary calculation suggests that the error in the flux balance is very low, 10^{-8} m^3/s. The average head at the interface is 27.7 m. The pressure solution for the whole region is shown in Figure 2-6. In Figure 2-7 the pressure in the repository-scale DFN region and in a layer of the adjacent CPM model is shown with a more restricted range to show the pressure variations around the repository-scale.

The Darcy velocity in the fracture network is shown in Figure 2-8 and Figure 2-9. These show two important results. Firstly, much higher velocities occur in the fracture zones due to better connectivity and a higher fracture transmissivity. Secondly, there is a lot of variability (7 orders of magnitude) in the magnitude of velocity in the fractures. This is unlikely to be captured in an upscaled SC model where a lot of this detail will be averaged out. Pathline calculations in the combined region were also carried out. Some illustrative examples for the pathline output as visualised in Avizier, are shown in Figure 2-10 and Figure 2-11.

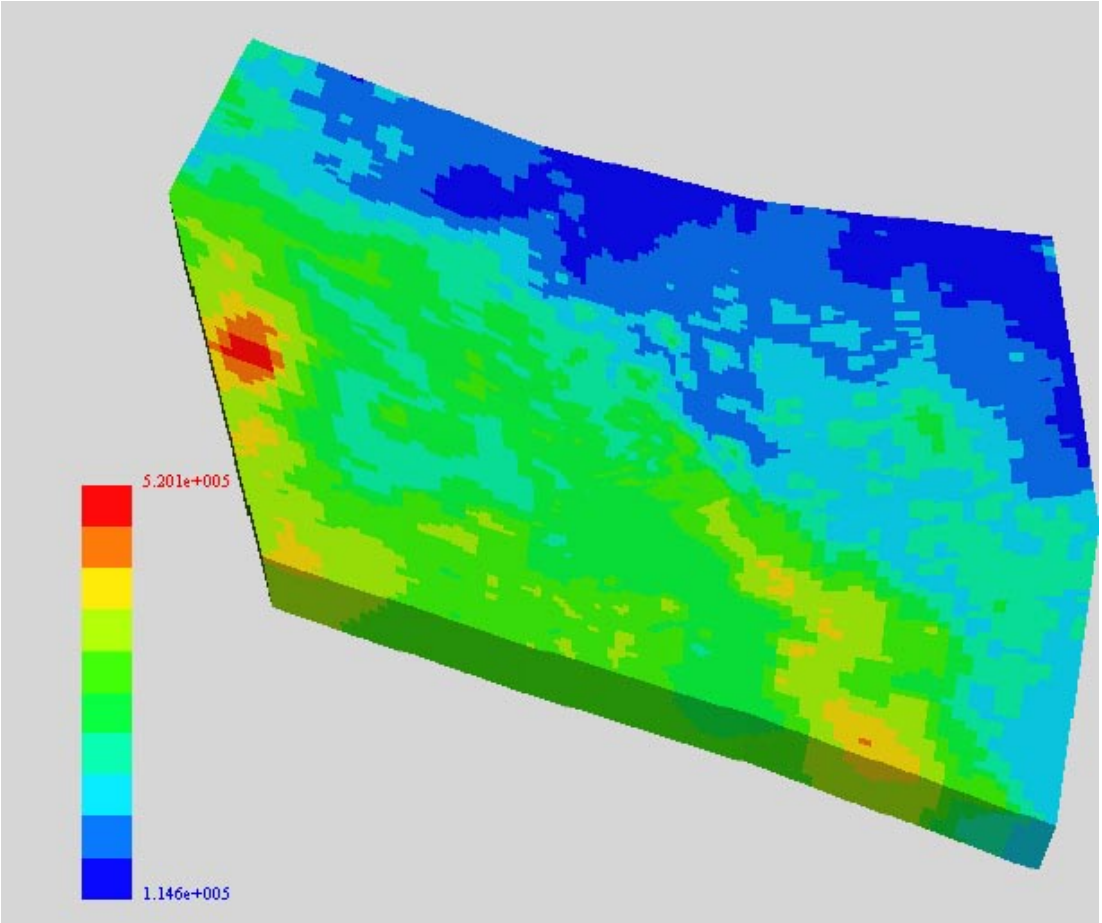

Figure 2-6. *Pressure distribution in the full region. The range of head values is 11-52 m.*

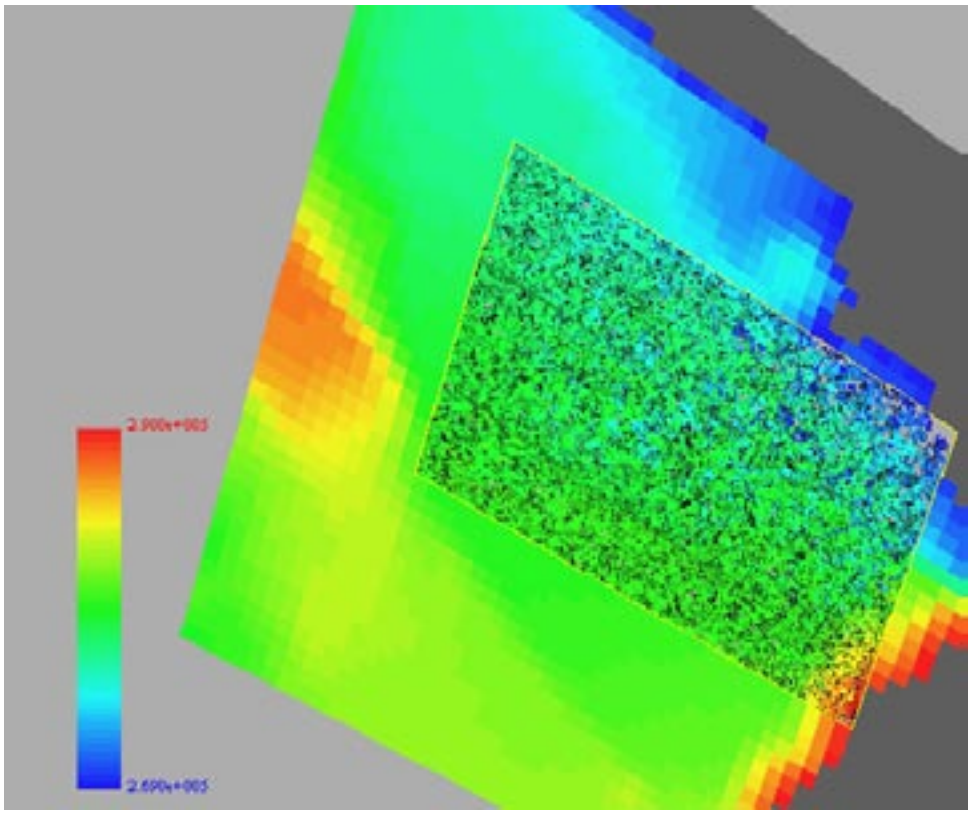

Figure 2-7. *Pressure distribution in the DFN region and local-scale CPM region. The head range here is only 26.9–29.0 m. The areas in black have pressures outside the range shown.*

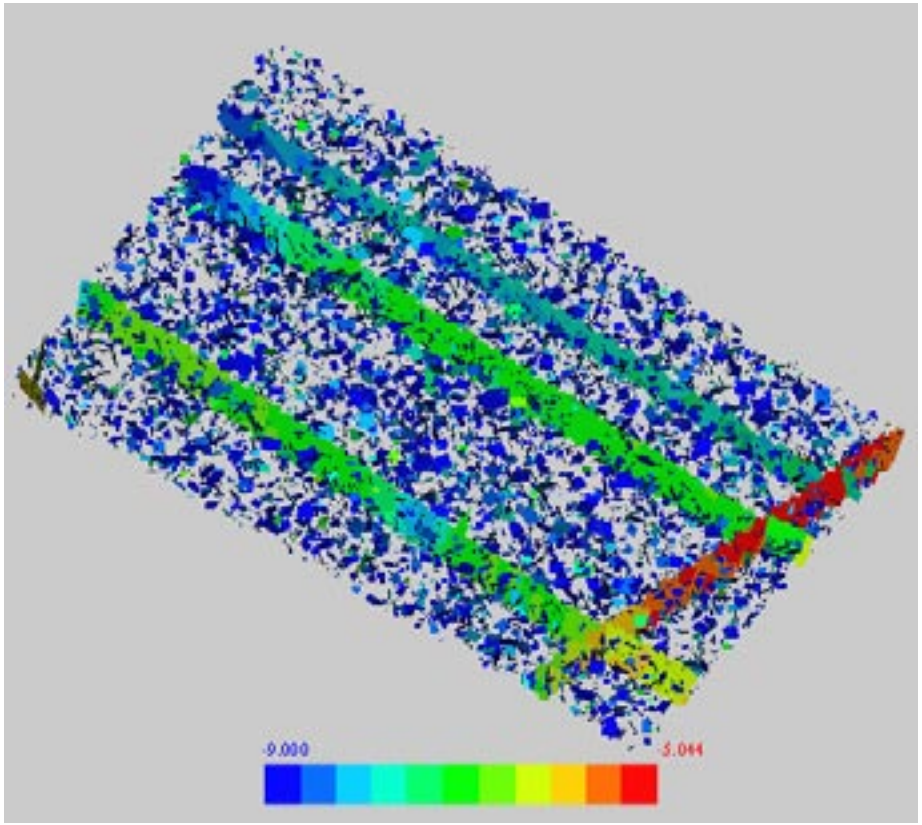

Figure 2-8. *Showing all fractures coloured by the Darcy velocities, in a logarithmic scale between 10^{-9} (blue) and $10^{-5.044}$ (red) m/s. The fracture zones can be clearly seen since the Darcy velocity in them is visibly larger than in the random fractures.*

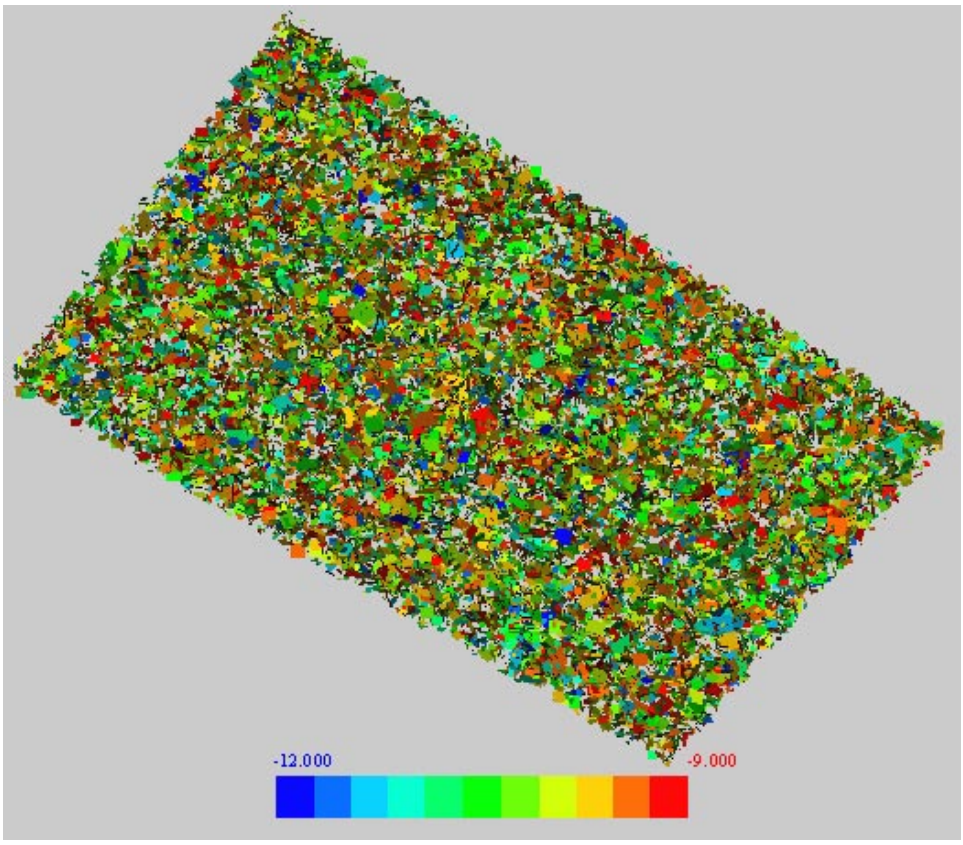

Figure 2-9. *As Figure 2-8 but showing fractures with lower magnitude Darcy velocity. 50% of the fractures with Darcy velocities in this scale are shown.*

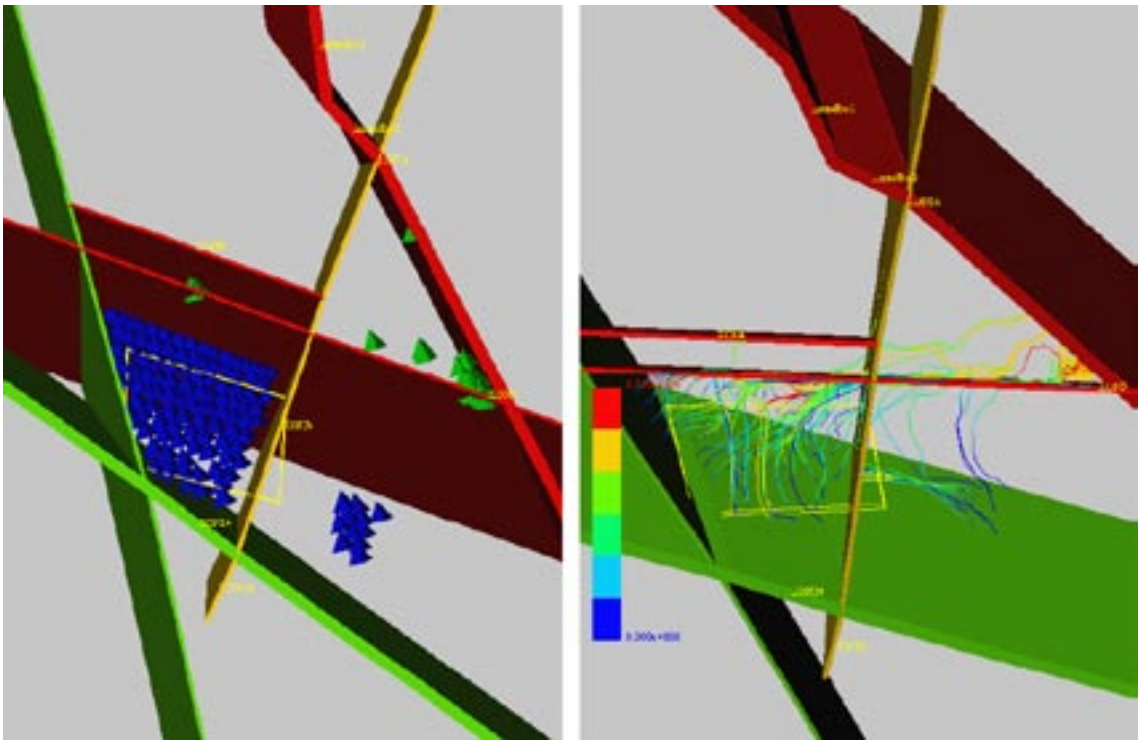

Figure 2-10. *Plan view of pathline as represented in Avizier. Left: start (blue) and end points (green). Right: full pathlines coloured by travel time. It can be seen how the particles released reach fracture zone 5 and then quickly move through it until they exit toward Imundbo.*

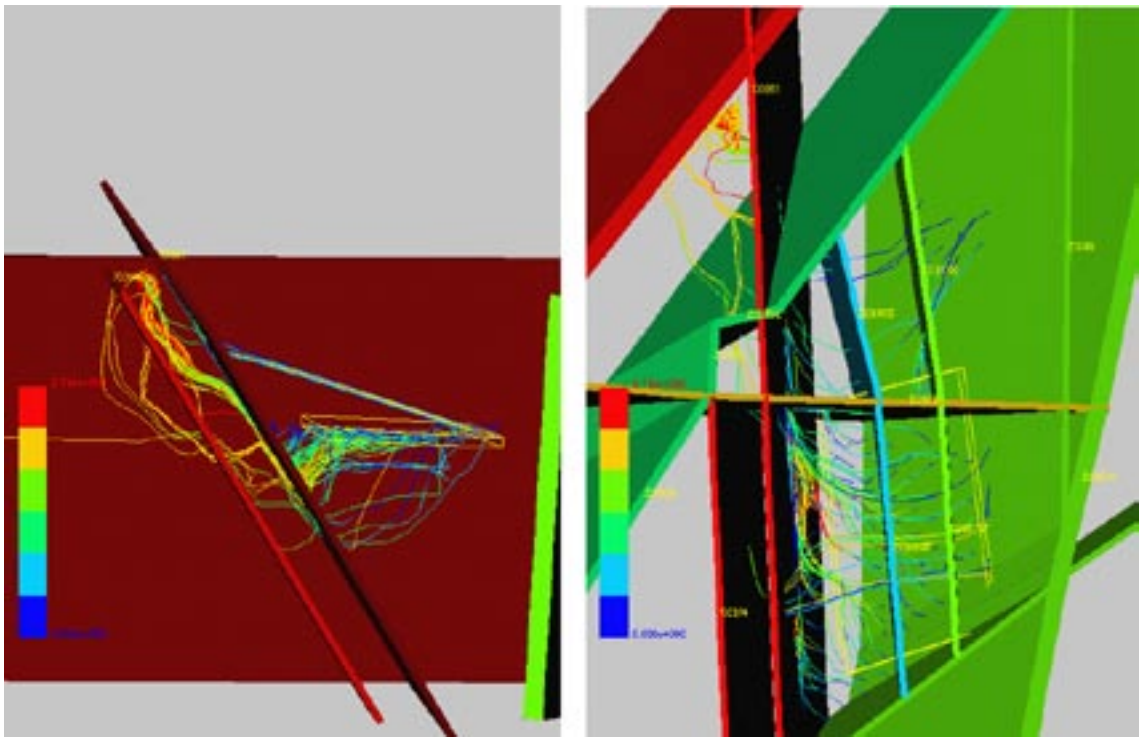

Figure 2-11. *Further examples of Avizier representation of pathlines starting from the DFN repository region (yellow box) and moving towards the large fracture zones in the CPM region. View from west (left), and plan view with local zones (right).*

Pathlines were started from 120 locations mostly in the DFN sub-model and then tracked through both DFN and CPM regions to the surface. The exit points were generally clustered together in a few places: Zone 5, or at the intersection of Zone 5 and Imundbo. Zone 5 was a very significant pathway for most particles. Though some paths starting in the south of the northern rock block follow the base of Zone 2.

2.2.1 Comments and conclusions

In the preliminary calculations a regional model of Beberg was used for the CPM part. The repository-scale region was modelled as a DFN. The randomly distributed fractures were included using Aberg fracture distribution data. In this way we tested the practical limits for this concept. Also using embedded grids it was possible to nest a more detailed site-scale model. The developed model was on the edge of what is practicable with current computer resources in terms of RAM and the current version of CONNECTFLOW. However, CPU requirements of about 1 hour per realisation imply that Monte-Carlo calculations using this model are feasible. Having a much larger DFN region would not be possible for the small-scale fractures important on the canister-scale. For the current fracture data, a site-scale DFN model would have many millions of fractures. However, for a hierarchical concept of fracturing on different scales it would be possible to reduce the DFN model by including the large and intermediate scale fractures in the local-scale and only having the small-scale fractures in the repository region. This was done with the small-scale fracture set in the AMP calculations to decrease the calculation load. However, for such an approach to be valid it must be established that flow on the site-scale is predominantly in the large and intermediate scale fractures. This was not the case in the AMP data as intermediate and canister scale fractures had the same transmissivity PDF parameters.

One interesting feature in NAPSAC that was not tested is the ability to model fracture zones geometrically as a plane and then generate a swarm of fractures around and centred on the plane. The concept gives much flexibility such as to model the mid-plane as a conductive feature or less permeable feature. Input data for the surrounding fracture swarm can be chosen from several distributions e.g. for orientation angles relative to the plane.

The workflow to set up a model in CONNECTFLOW is straightforward. This demonstration benefited of using a previously defined regional model and using Aberg data for the DFN. To create a model in CONNECTFLOW if these parts are available is not very time consuming.

2.2.2 Additional work within Task 1

It is acknowledged that the location of the DFN part should be adjusted to cover the whole of the Northern Rock block at repository level. Further work would be beneficial to check the consistency of permeability between CPM versus DFN, to further visualise the results for verification purposes and present the concept, and to update the fracture data. The motive for updating the fracture data in the DFN part is that recent studies (TR-01-21 and ITD-00-03) may have produced higher quality data. Most of this work is made within Task 2.

It should be noted that as part of Task 1, CONNECTFLOW and the developed models have been installed on the Kemakta Linux machine Urax.

3 Simulation of canister flows and transport for a nested DFN/CPM model of Beberg

Based on Task 1 models, Task 2 was initiated to demonstrate how the CONNECTFLOW concept could be applied to site assessment modelling and to show what results can be obtained. In particular, calculations of flow rates and transport statistics are calculated and compared to earlier porous medium models of Beberg to demonstrate both consistency and what extra information can be obtained.

Prior to running a set of realisations, consistency of the permeability of the SC based on Beberg data and the DFN model based on Aberg was checked. The approach taken was to use the flux-based upscaling method in NAPSAC to obtain the equivalent SC permeability for the AMP fracture network data. The fracture transmissivity data was then adjusted to give a DFN region that has the same equivalent permeability (mean and standard deviation) as the SC data used at Beberg for 35 m cells. Hence, the fracture transmissivity data from Aberg was rescaled to ensure self-consistency with SC permeability model for Beberg. This is an example of the benefit of having both approaches, CPM and DFN in a single package, as it is easy to check consistency in the data used for either concept.

Twenty realisations of the nested model were performed to sample the variability in performance measures such as canister flux and transport statistics. The results were then compared with the SR 97 results based on a SC approach in HYDRASTAR.

3.1 Permeability consistency

Based on the work related to constructing the CONNECTFLOW model and preliminary calculations in Task 1, the permeability field was checked within the DFN domain. The aims were to compare with reported data from Beberg and to match the SC values. Figure 3-1 illustrates random fractures based on the input data.

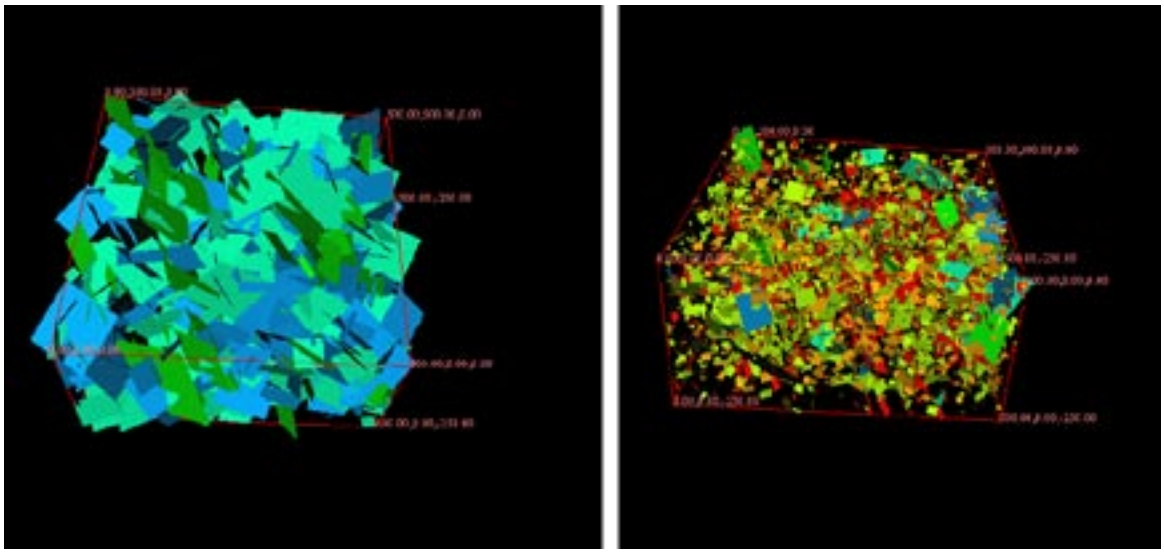

Figure 3-1. *Left, the set of larger fractures, and right, 10% of all fractures.*

Two scales of fractures are considered: the small-scale and a lower density intermediate-scale defined by the data in Table 2-2 and Table 2-3. In NAPSAC, a domain (500×500×250 m) was created with random fractures based on the AMP data. Using the NAPSAC upscaling capability the domain was divided into 25, 50 and 100 m sub-regions and the full permeability tensor was calculated for each one of the sub-regions. The upscaling method is illustrated in Figure 3-2.

From the calculated permeability tensor the principal permeabilities (major, intermediate and minor K_{major}, K_{int}, K_{minor}) are obtained. The geometric mean of permeability, K_g, for each sub-region was calculated as

$$K_g = (K_{major} \cdot K_{int} \cdot K_{minor})^{1/3}.$$

Here, permeability is denoted K [m^2], and conductivity is denoted k [m/s]. The relationship between them is

$$K = k\mu/\rho/g$$

where μ is viscosity, ρ is density and g is the gravitational acceleration. The obtained mean permeability value for the sub-regions was compared to the CPM domain and adjusted for consistency.

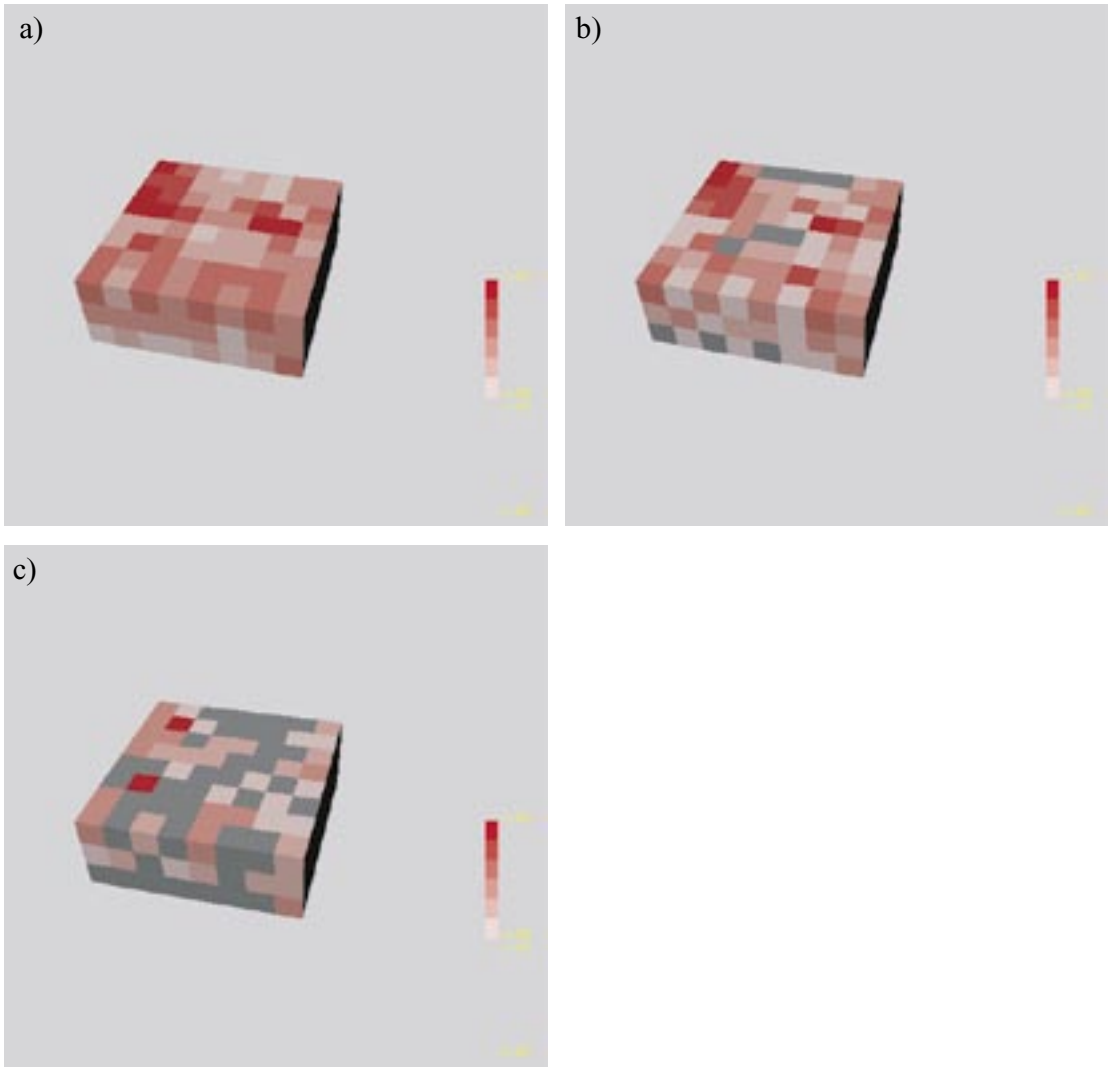

Figure 3-2. *Permeability tensors for the sub-regions for 50 m blocks, a) K_{major}, b) $K_{intermediate}$ and c) K_{minor}. Each sub-region is coloured according to logarithmic permeability. Red for high permeability, pink for low.*

3.2 Derivation of F-quotient in CONNECTFLOW

One of the transport parameters that is required in an assessment is the F-quotient. It is important since it is dependent on the degree of channelisation in the fracture network and is important for transport processes such as matrix diffusion and sorption. Conceptual models have been developed in other projects for deriving the F-quotient for both DFN and CPM models. However, in the context of a nested DFN/CPM model it is important that a self-consistent model is applied to both concepts where they coexist. The implementation in CONNECTFLOW is that the F-quotient is calculated for each 'leg' along each transport pathway. A leg in the DFN region is a path along a fracture plane between two fracture intersections. In the CPM region a leg is a section between two points on a pathline and is usually the part between two faces of a finite-element, though this may be discretised further. The F-quotient for each leg is calculated as follows:

CPM: $F_i = ar_i * dx_i / q_{i,}$

DFN: $F_i = 2t_i / e_{i,}$

For CPM, ar_i is the fracture surface area per unit volume in the finite-element, dx_i is length along the current section of path, q_i is the specific discharge. Note, ar_i can be calculated as an equivalent upscaled property for a given sub-volume in a DFN model, much in the same way that the equivalent fracture permeability is calculated. For DFN, t_i is the travel time along the path in the fracture, and e_i is the transport aperture of the fracture. Thus, the F-quotient along an entire pathway is the sum, ΣF_i, of the individual F-quotients for each leg.

3.3 Performed simulations

Once the model, consisting of a CPM domain, a DFN domain and boundary conditions, had been fine-tuned, a number of realisations were performed. The CPM domain was stochastic and an embedded grid was used. Pathline calculations were made for each of the 20 realisations. The number of pathlines in each realisation was 120. The target depth for the starting positions is –604.5 m below sea level. About 55% of the pathlines start within the DFN part, the others starting from the CPM part. Pathlines starting in the DFN part are released in the nearest fracture. In some fractures the flow rate is very low or negligible so released particles may travel very slowly or even stay immobile in such cases. Unless the tunnel construction has induced additional fractures, this may be a real case scenario. A number of options on how to handle pathlines starting in relatively impermeable rock may be studied in the future.

3.3.1 Performance measures

As performance measures of the simulated host rock for a repository, groundwater travel times, t_w [yrs], flux at starting positions, q_c [m/yrs], and F-quotients for flow paths, F [yr/m], are shown in Table 3-1. In addition statistics of path lengths are given. Label "Total" indicates the subset of the 120 pathlines that do not get stuck near the release point. Label "Top" indicates pathlines that reach the top surface of the model.

The results suggest that the median travel time is 47 years, with an inter-quartile range from 14 to 135 years for the pathlines reaching the top surface. About 15% of the pathlines fail to exit at the top surface of the model. The variance of $\log_{10}$ travel times in the CONNECTFLOW model is 0.7. The corresponding results from the base case of the Beberg site-scale simulation /Gylling et al. 1999/ are average travel times of 56 years, with an inter-quartile range from 29 to 104 years. In the HYDRASTAR simulation the

Table 3-1. Statistical summary for 20 realisations of 120 starting positions with a flow porosity of $\varepsilon_f = 10^{-4}$.

Statistical entity	$Log_{10}(t_w)$ Top	$Log_{10}(q_c)$ Total	$Log_{10}(F)$ Top	$Log_{10}(L)$ Top
Mean	1.630	–2.854	5.618	3.515
Median	1.669	–2.736	5.663	3.510
5th percentile	0.291	–4.565	4.215	3.282
25th percentile	1.150	–3.401	5.146	3.410
75th percentile	2.131	–2.124	6.150	3.600
95th percentile	2.791	–1.287	6.792	3.770
St deviation	0.809	1.205	0.814	0.148
Variance	0.654	1.453	0.663	0.022
Min value	–1.326	–10.233	2.646	3.154
Max value	6.989	–0.052	10.655	4.034
Fraction	0.849	1.000	0.849	0.849

variance of $\log_{10}$ travel times is 0.2. Note that 100 simulations were performed in the base case of Beberg in SR 97. These results demonstrate good consistency in the mean travel time with SR 97, but as might be expected from DFN model the variance is a lot higher. The standard deviation in travel time is about a factor of 3 higher. This may partly be a result of the relatively few realisations performed here. However, it shows that using a DFN model with a more detailed representation of canister-scale flows can lead to significantly greater variability in transport statistics, and that may have implications for safety assessment. The distribution of travel times is shown in Figure 3-3.

Furthermore, the results suggest that the median flux at starting positions is $1.8 \cdot 10^{-3}$ m/years, with an inter-quartile range from $4.0 \cdot 10^{-4}$ to $7.5 \cdot 10^{-3}$ m/years for all pathlines. In Figure 3-4 the distribution of q_c is shown. The variance of $\log_{10}$ flux values for Task 2 is relatively high, 1.5. The corresponding results from the base case of the Beberg site-scale simulation are: a median flux of $1.2 \cdot 10^{-3}$ m/years, with an inter-quartile range from $4.8 \cdot 10^{-4}$ to $3.0 \cdot 10^{-3}$ m/years /Gylling et al. 1999/. The variance in SR 97 is 0.4 for the $\log_{10}$ flux values.

Using the recently developed feature in CONNECTFLOW, calculations of F-quotients are made. In SR 97 F-values had to be estimated as $F = t_w \cdot a_r / \varepsilon_f$, where a_r is the flow-wetted surface per volume of rock and ε_f is the flow porosity, whereas in the prevailing study, F-values are calculated directly in the code. In the DFN domain of the model the F-values are based on locally calculated properties, i.e. one F-value for each fracture segment traversed is obtained. In the CPM domain the F-value has to be approximated and based on an assumed value of a_r. Throughout the CPM domain $a_r = 1.0$ is used as in SR 97. However, in CONNECTFLOW one F-value for each transport leg (i.e. either a finite-element or a fracture plane) is obtained. The total F-quotient for a single path is the sum of individual F-values. The distribution of F-quotients is shown in Figure 3-6.

If we again use the base case in SR 97 as a reference, the following F-quotients can be used as comparison for the 100 realisations of 120 starting positions and by assigning the flow porosity to 10^{-4} and a_r to 1.0 m^{-1}. The median $\log_{10}$ F was 5.752, the 5^{th} percentile was 4.982 and the 95^{th} percentile was 6.367. The variance of $\log_{10}$ F was 0.203.

The distribution of the path lengths indicates that on average particles pass through about 3,200 m of rock on their way up to the surface. That distance is about five times the depths under the surface, i.e. the particles are not going straight up. The distribution is relatively narrow.

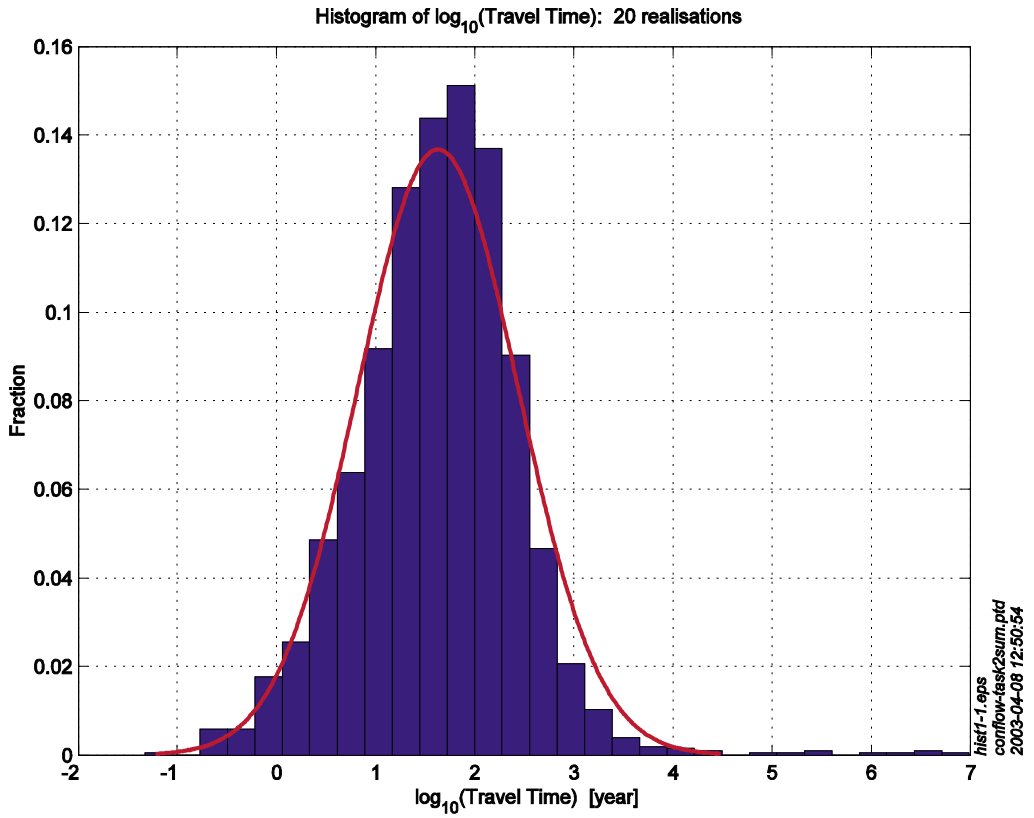

Figure 3-3. *Histogram of travel times for 120 starting positions in 20 realisations. A flow porosity of 10^{-4} is used.*

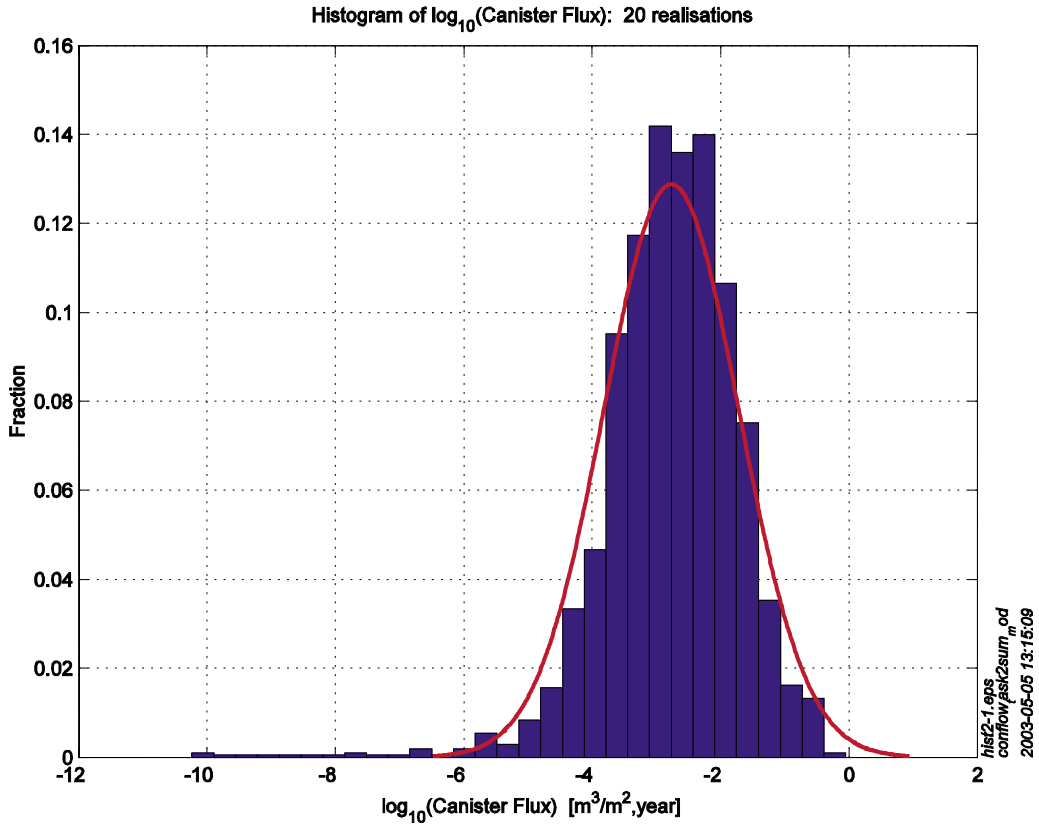

Figure 3-4. *Histogram of flux at 120 starting positions in 20 realisations.*

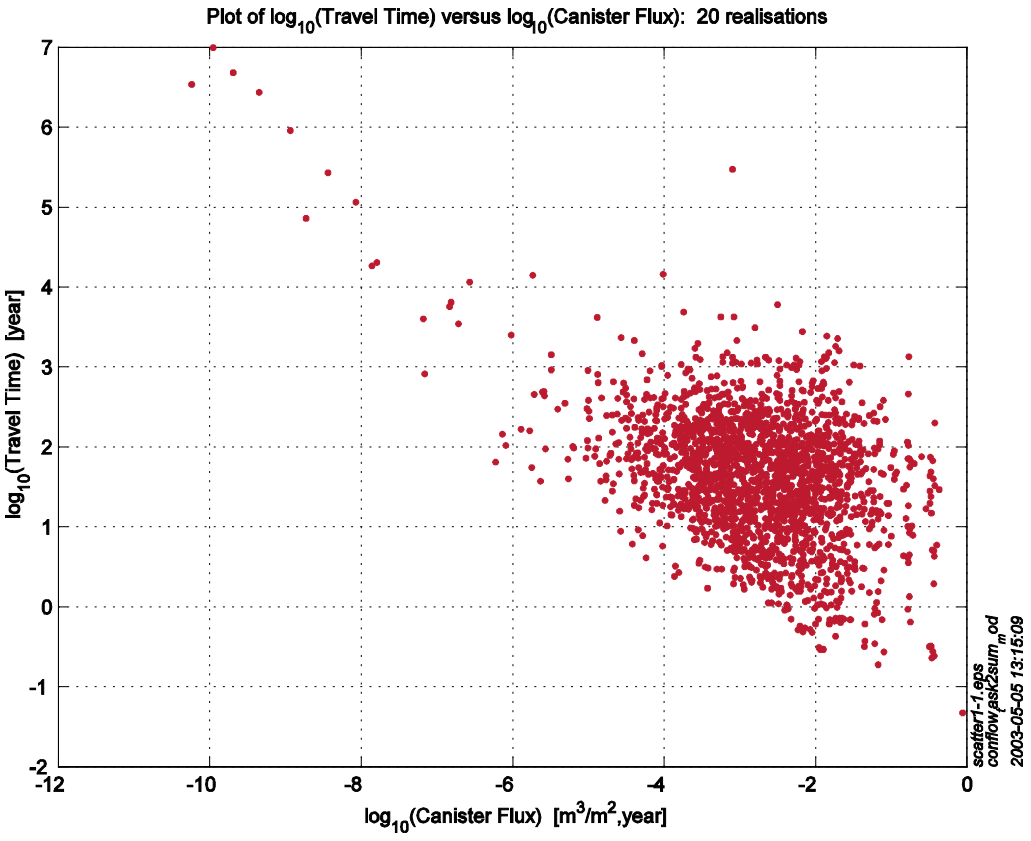

Figure 3-5. *Travel time [year] versus specific flow [m/y] at 120 starting positions of 20 realisations. A flow porosity of 10^{-4} is used.*

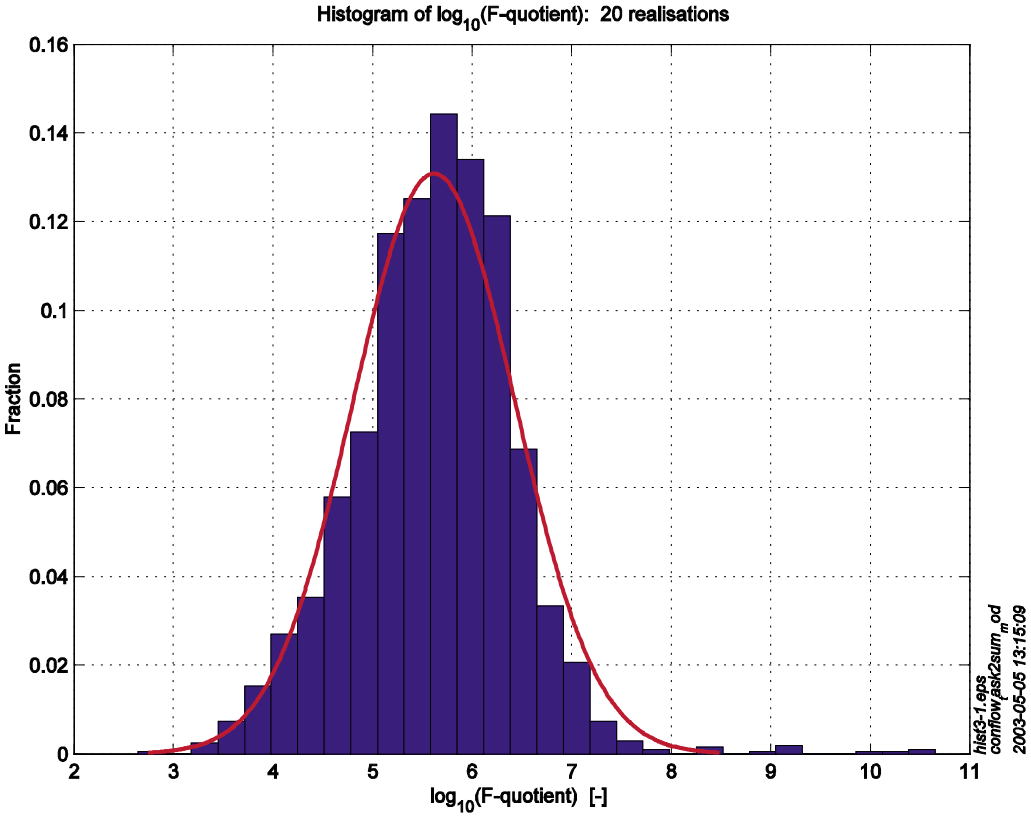

Figure 3-6. *Histogram of F-quotient values for 120 starting positions in 20 realisations. A uniform flow-wetted surface of 1.0 m^2/m^3 is used in the CPM domain.*

3.3.2 Validation of modelling results

To check that the flow solution is acceptable, the inner flux balance between the DFN and CPM domain is recorded in each realisation. This is shown in Table 3-2 for five realisations only. The flux balance varies between realisations, but is good in all cases, and is certainly an improvement on manual methods of nesting.

In order to study if Monte Carlo stability is reached accumulated medians are calculated of performance measures. In Figure 3-7 below the accumulated median of travel times is shown and in Figure 3-8 the accumulated median of flux at starting positions is shown. The ensemble statistics appear to be converging, but more realisations would have to be made before it is possible to say that Monte Carlo stability is reached. However, since our primary interest in this project is just to demonstrate the concept no more realisations are made.

Table 3-2. Flux balance between DFN and CPM domains for five realisations.

Realisation	1	2	3	4	5
Total flux from DFN to CPM, kg/s	27.4194	28.7021	30.1077	27.2458	26.4431
Total flux from CPM to DFN, kg/s	–27.4397	–28.7020	–30.1077	–27.2501	–26.4432
Net flux from DFN to CPM, kg/s	–0.0203	0.0001	0.0000	–0.0042	–0.0001
Estimated error, %	0.0741	–0.0003	0.0000	0.0156	0.0003

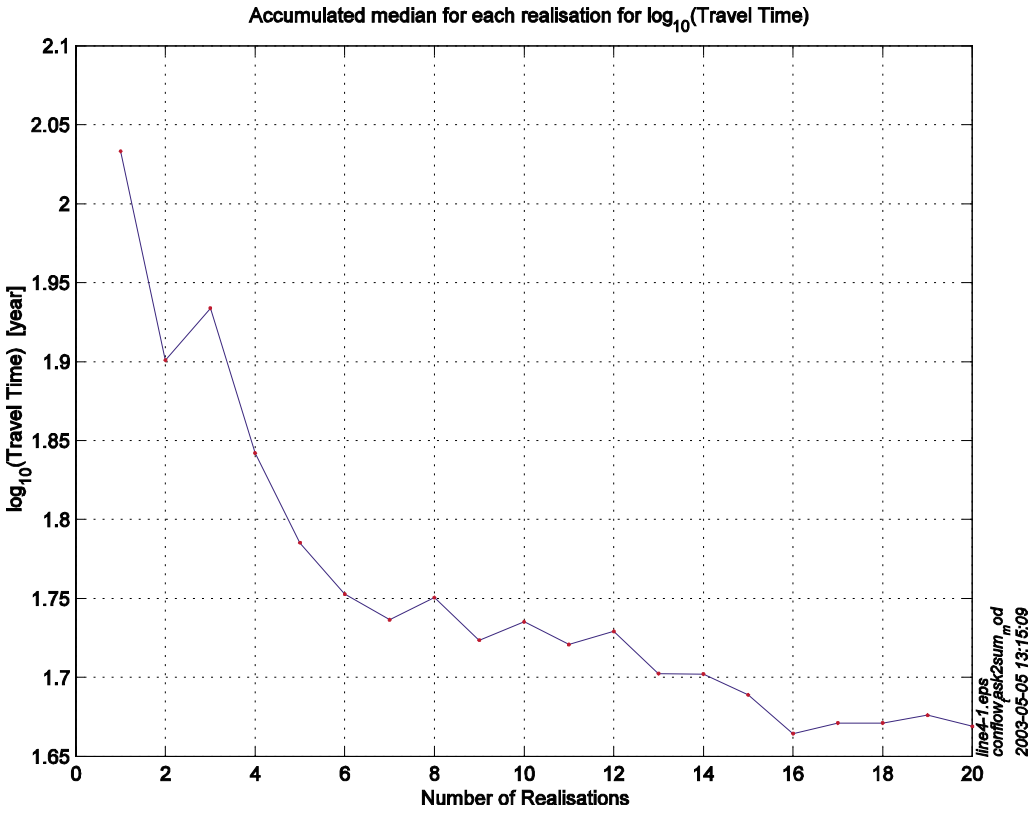

Figure 3-7. *Monte Carlo stability of median travel time versus number of realisations. Results for 120 starting positions and 20 realisations.*

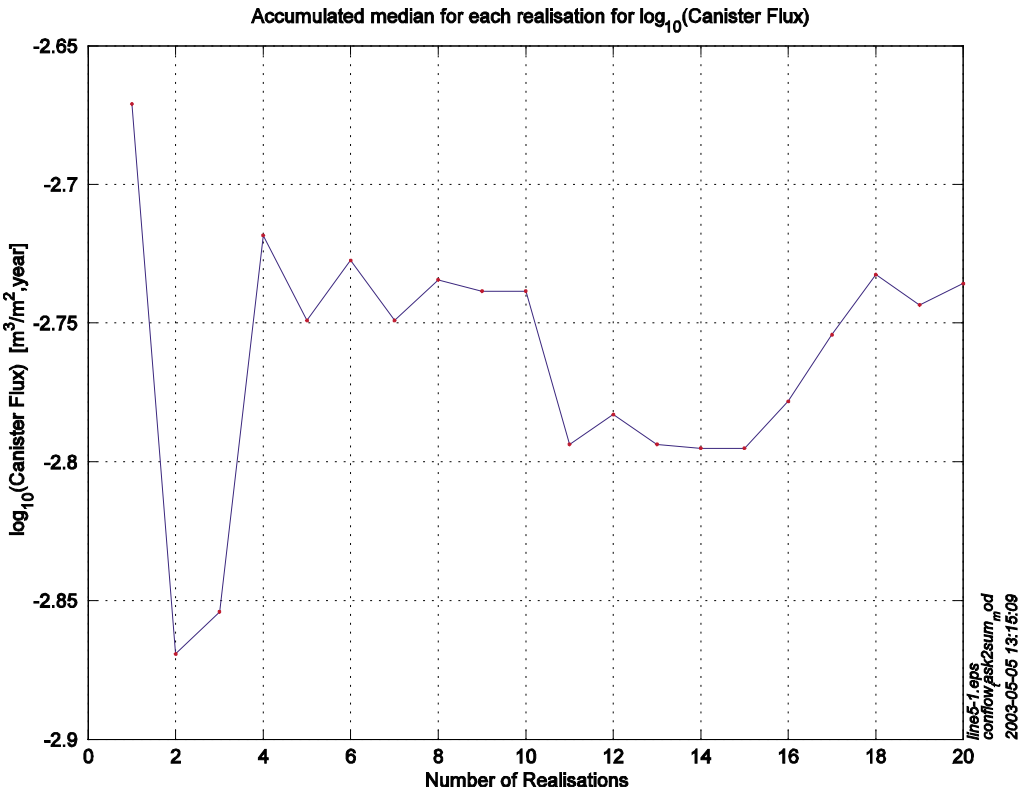

Figure 3-8. *Monte Carlo stability of median canister flux versus number of realisations. Results for 120 starting positions and 20 realisations.*

3.3.3 Canister location process

Since the criterion of abandoning a canister location is not defined, the analysis is here based on statistics and specific starting positions. Cumulative distributions of specific flow rates and travel times can indicate how many starting positions that have to be moved to more satisfactory locations. In addition, illustrations are made to further characterise the modelled starting positions.

In Figure 3-9 the cumulative distribution of specific flow at representative canister locations is shown. The total number of starting positions in the five realisations is used as reference. Based on the ensemble results and the used input data, and applying a value, say $q_c = 10^{-2}$ m/year as the threshold, about 25% of the deposition holes would be moved to a more suitable position. The reason that the cumulative curve does not reach unity is that about 2% of the specific flow values are discarded due to numerical reasons.

If the threshold of groundwater travel time is e.g. $t_w = 10$ years for accepting a canister location less than 15% of the deposition holes need to be moved. Again, the total number of starting positions in the five realisations is used as reference. This is shown in Figure 3-10. The reason that the cumulative curve does not reach unity is that about 12% of the pathlines fail to exit at the top surface of the model.

In the base case for site-scale simulations of Beberg in SR 97 some correlation between groundwater travel time and the specific flow may be observed /Gylling et al. 1999/. A similar plot is shown in Figure 3-11. Compared to SR 97 the correlation seems to be weaker. However, here are just five realisations made, whereas 100 realisations were made in SR 97.

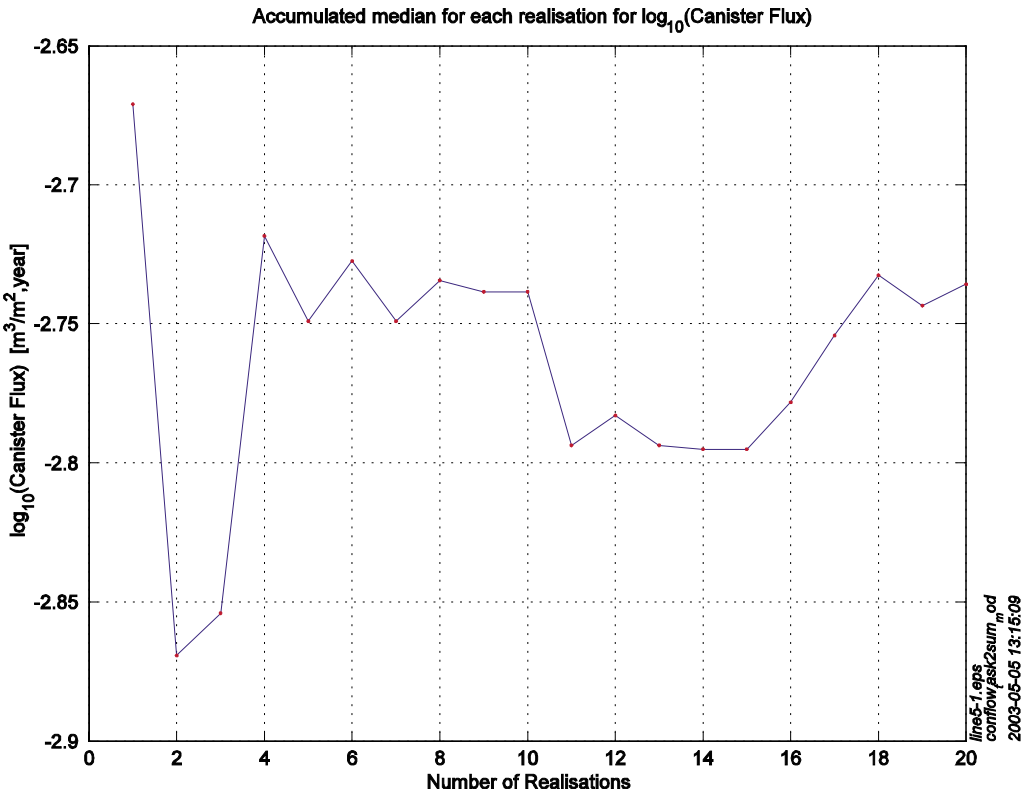

Figure 3-9. *Cumulative fraction of total number of starting position for specific flow [m/y] at representative canister locations.*

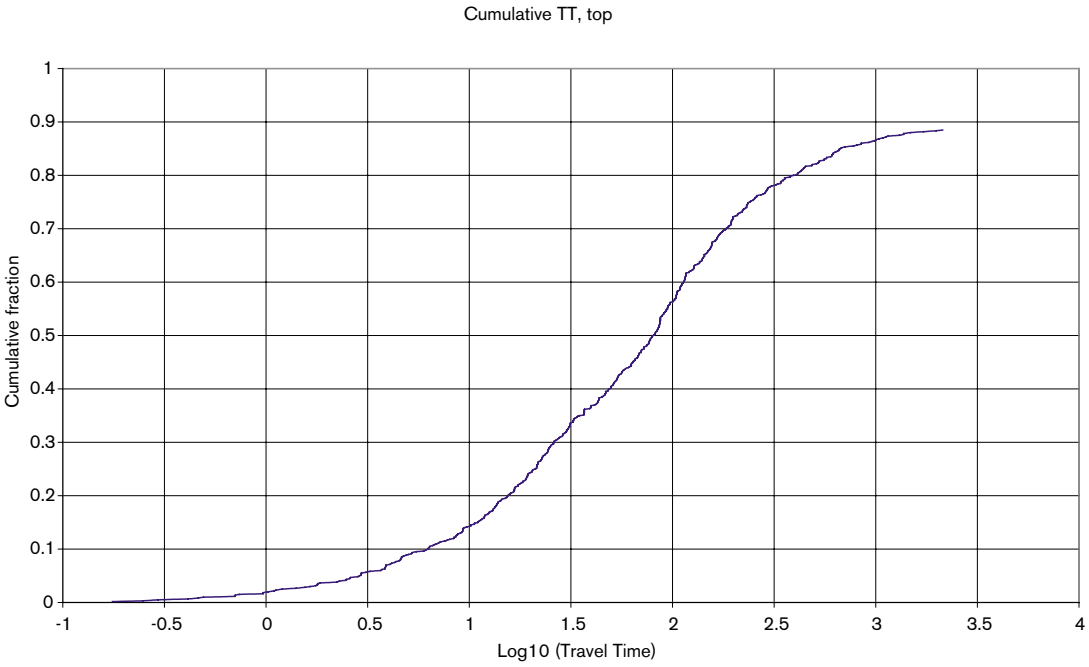

Figure 3-10. *Cumulative fraction of total number of starting position for groundwater travel time [year] at representative canister locations. Based on 120 starting positions in each of the 5 realisations, and flow porosity 10^{-4}.*

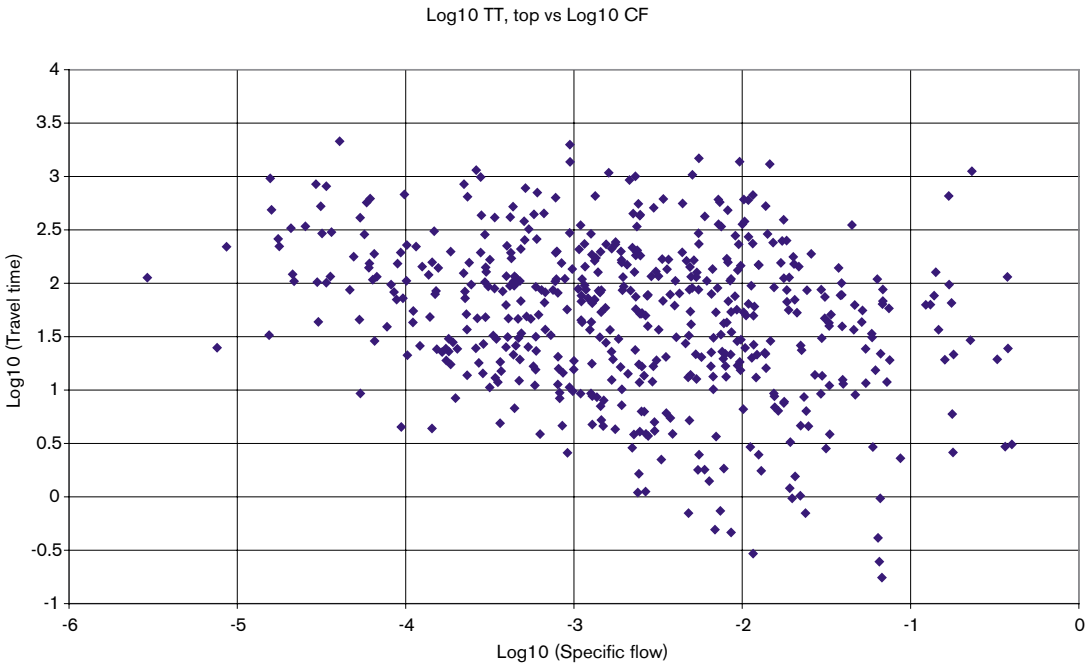

Figure 3-11. *Travel time [year] versus specific flow [m/y] at 120 starting positions of 5 realisations. A flow porosity of 10^{-4} is used.*

To further characterise the starting positions based on travel time Figure 3-12 is made. The results shown in Figure 3-12 suggest that paths starting near positions 20, 62 and 106 tend to give short travel times. Position 20 is located in the southern corner of the Northern block, position 62 is near the eastern corner, and position 106 is near the northern corner of the same block. Position 20 and 106 are both relatively near Zone 1, whereas position 62 is closer to Zone 5 and Zone 12. In the base case for the site-scale modelling of SR 97, travel times for particles released near position 20 resulted in short travel times as well.

3.3.4 Enhanced modelling output

As a note CONNECTFLOW generates additional information that is not currently used in far-field modelling. This includes data such as how the pathline is distributed between the domains. Table 3-3 below is included as an illustration. It shows contributions to the performance measures for a single pathline (number 12) from the domains (DFN and CPM rock types) in one realisation. This type of information is taken from the standard CONNECTFLOW output file. Apparently, path 12 starts in DFN (FRACTURED ROCK), continues in CPM (BZN2L2), goes back in DFN and then again back to CPM. Hence, transport statistics could be derived for the individual rock domains rather than for just the whole path. To the far right in the table two columns are added to illustrate contributions as percentage for the performance measures t_w and F-quotient for this particular path in this realisation.

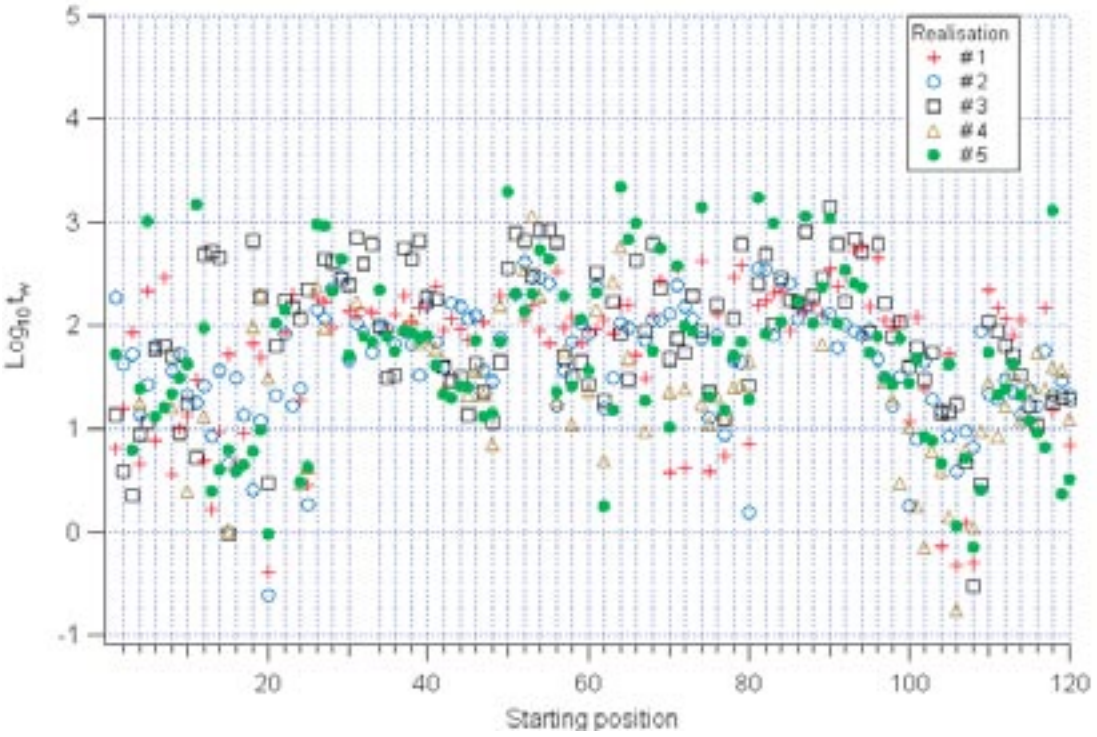

Figure 3-12. *Groundwater travel time versus starting position for 5 realisations and a flow porosity of 10^{-4}.*

Table 3-3. Some performance measures along the pathline for path number12.

ROCK	Time [yr]	Pathlength [m]	F-quotient [Yr/m]	Average velocity [m/yr]	Rock Name	Fraction time, %	Fraction F, %
11	4.19E–01	3.75E+00	2.80E+03	8.93E+00	FRACTURED ROCK	3.52	6.62
8	1.78E–02	2.65E+01	3.72E+02	1.49E+03	BZN2L2	0.15	0.88
11	1.13E+01	5.41E+01	3.76E+04	4.80E+00	FRACTURED ROCK	94.98	88.93
8	1.61E–02	1.99E+01	1.79E+01	1.23E+03	BZN2L2	0.14	0.04
7	1.43E–01	1.73E+03	1.48E+03	1.20E+04	BZN2L1	1.20	3.50
2	7.63E–04	5.48E+01	7.12E+00	7.18E+04	BZN2R1	0.01	0.02
1	4.42E–04	7.28E+01	4.45E+00	1.65E+05	NSRFR1	0.00	0.01

3.3.5 Test of F-quotients calculations

To check the calculations of F-quotients a single simulation was performed using a pure CPM domain. In fact, the same model is used as a reference case in Task 4. The reference case was used to check the developed approach to calculate F-quotients. Based on the results from the CPM model in the reference case a comparison is made between the F-values calculated directly in the code and F-values calculated as in SR 97. In SR 97, F-quotient values were estimated as $F = t_w \cdot a_r/\varepsilon_f$. In the reference case $a_r = 1.0$ m^2/m^3 and $\varepsilon_f = 10^{-4}$ are used and properties of the simulated host rock. The same values are used in the SR 97 type of estimation, and t_w are taken from the CPM simulation. As may be observed in Table 3-4 the results appear to be very similar. In a more realistic simulation the material properties of the host rock follow some spatial variation. Then this type of comparison would show much greater difference.

Table 3-4. Comparison of log_{10} F-quotient values calculated directly in CONNECTFLOW with F-values estimated using the method proposed in SR 97. The number of starting positions is 192.

Statistics	Log_{10} F calculated in CONNECTFLOW	Log_{10} F calculated as in SR 97
Average	4.55	4.55
St dev	0.78	0.78
Variance	0.61	0.61
Median	4.18	4.17
Min	3.38	3.38
Max	6.03	6.02

An additional test was made by modifying the value of the flow-wetted surface value for the rock mass keeping the value for the fracture zones. The issue is to observe the impact of this on the calculation of the F-quotient. In the Task 2 simulations a uniform value of the flow-wetted surface is used. In this test the value for the rock mass is multiplied with 0.1. In Table 3-5, a comparison of log10 F-quotient for a case with uniform $a_r = 1.0$ m^2/m^3 and a case with $a_r = 0.1$ m^2/m^3 for the background rock mass, is given.

It may be seen that the median and the minimum values are less in this variant compared to the uniform case, whereas the other statistical values differ quite little. The low difference may be explained by that most of the pathlines spend most of the way in fracture zones. The values for the fracture zones are not modified. Also, the values calculated for the fractures in the DFN domain are carried out in the same way in the two cases.

Table 3-5. Comparison of log10 F-quotient for a case with uniform $a_r = 1.0$ m^2/m^3 and a case with $a_r = 0.1$ m^2/m^3 for the background rock mass but otherwise identical.

Statistics	Log_{10} F calculated in CONNECFTFLOW Case: Uniform a_r	Log_{10} F calculated in CONNECFTFLOW Case: Lower a_r for rock mass
Average	5.92	5.05
St dev	1.12	1.05
Variance	1.25	1.10
Median	6.04	5.18
Min	3.67	2.82
Max	10.67	10.58

4 CONNECTFLOW repository-scale model

A second generic application of CONNECTFLOW is to nest a canister-scale CPM sub-region within a DFN model of the repository-scale fractures. An explicit CPM model of the repository back-filled tunnels, deposition holes and plugs nested within a detailed DFN model can be used to represent the effect of different designs, such as back-fill permeability and repository geometry, as well as the interaction with flow in discrete fractures. In this section we report the development and testing of such a model that with the project was called Task 3. The resulting model was further developed within Task4 for the purpose of illustrating the types of results that can be obtained from such a model and how these may be used to provide more realistic input to near-field models.

For the purposes of illustration, DFN data from Aberg is used. This is the same approach as in Task 1 though the model was positioned in a Beberg model. The model is generic in terms of the basic application. The maximum size of the model that can be constructed depends on concept and site-specific data. The model produced in Task 3 could later be modified for the shaft and ramp (incline) study that has recently been initiated at SKB.

4.1 Modelling approach

In Task 3 a rather complex CPM model representing a tunnel system is nested within a DFN model. The tunnel system includes a number of deposition tunnels and six access tunnels. Each deposition tunnel has deposition holes according to the concept of KBS-3 vertical. The resulting CPM elements are then nested into a DFN model using Aberg data. The challenge for this task is to create the inner boundary conditions i.e. to couple the DFN fractures to the CPM elements. Compared to a SC model the concept may be used to give better and more detailed input data to the COMP23 near-field model since flows through the engineered structures (tunnels, roadways and deposition holes) are represented explicitly. The representation of a system of 6 tunnels extending from a section of roadway is shown in Figure 4-1.

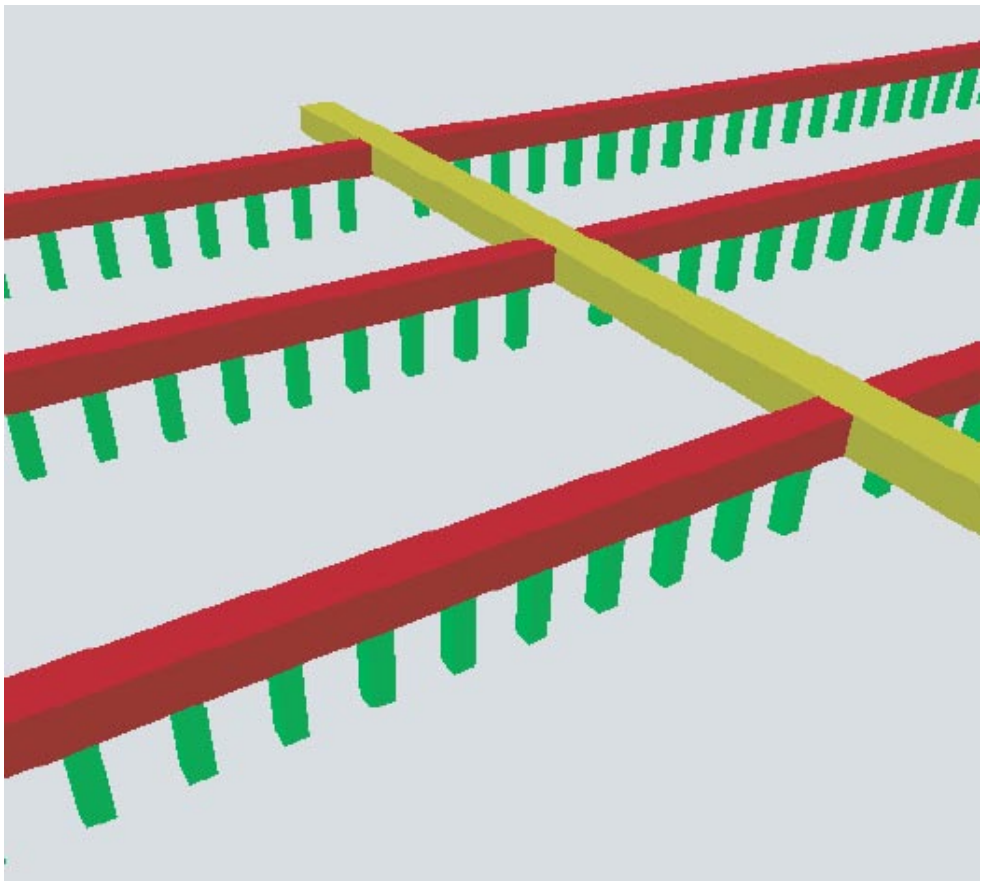

Figure 4-1. *The CPM model with tunnels (red), roadway (yellow) and canisters (green) is shown in more detail here. Each tunnel contains 32 deposition holes. The grid was created with the finite-element-mesh generator FEMGV.*

As input data to the tunnel system information from SR 97 was used. A sub-set of six deposition tunnels was used and connected by an access tunnel, according to the Beberg layout of SR 97 /Munier et al. 1997, see Appendix A/. To create the tunnel system the tool FEMGV was used. FEMGV is a CAD application that may be used to create a finite-element mesh. Meshes generated with FEMGV can be imported into CONNECTFLOW via an existing interface. Different parts of the mesh were assigned to different materials in FEMGV, e.g. tunnel, canister, roadway, fractured rock. When importing the FEMGV mesh it is then necessary to assign each material to being either part of the NAMMU sub-region or NAPSAC sub-region. The resulting mesh and the engineered parts represented by a NAMMU porous medium model are shown in plan and oblique views in Figure 4-2 and Figure 4-3. The fractures in the DFN part of the model are shown in Figure 4-4. This shows that the network of small-scale fractures is dense and connected. More information on the location of the tunnel system and creation of the mesh is given in Appendix A.

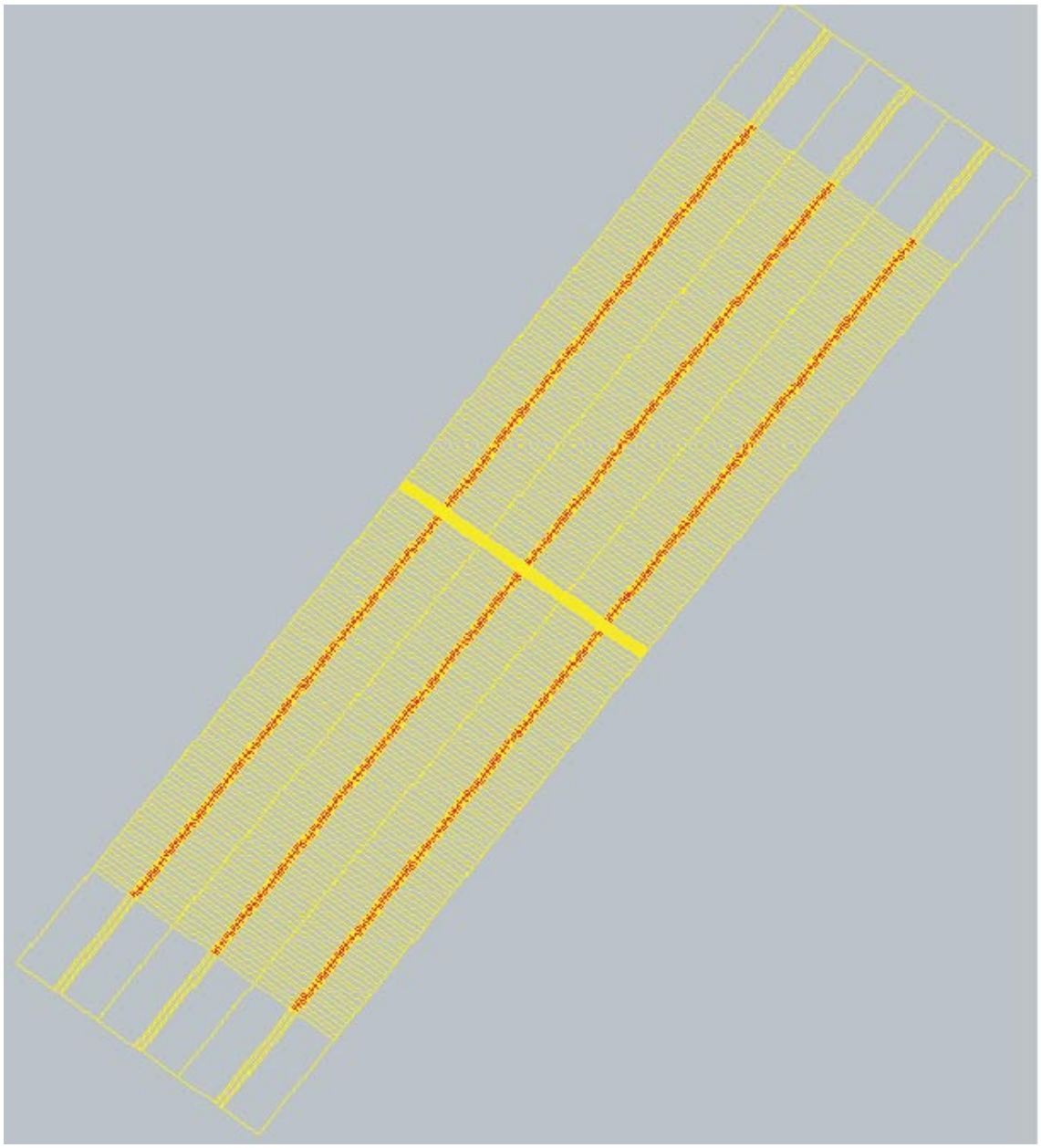

Figure 4-2. *Plan view of the grid used to model the canister-scale model.*

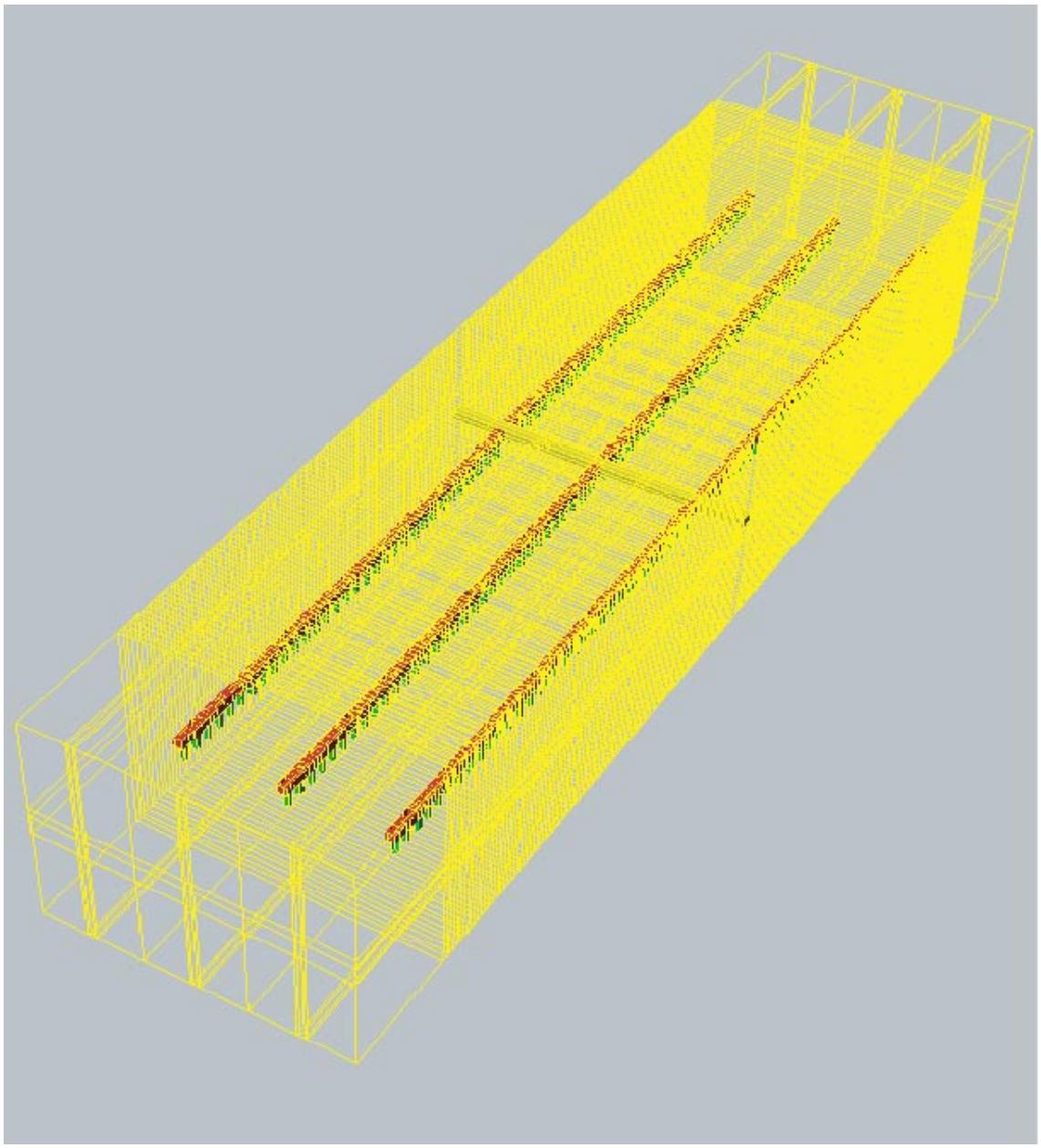

Figure 4-3. *Oblique view of the mesh used for the canister-scale model showing the tunnels (red), roadway (yellow) and canisters (green).*

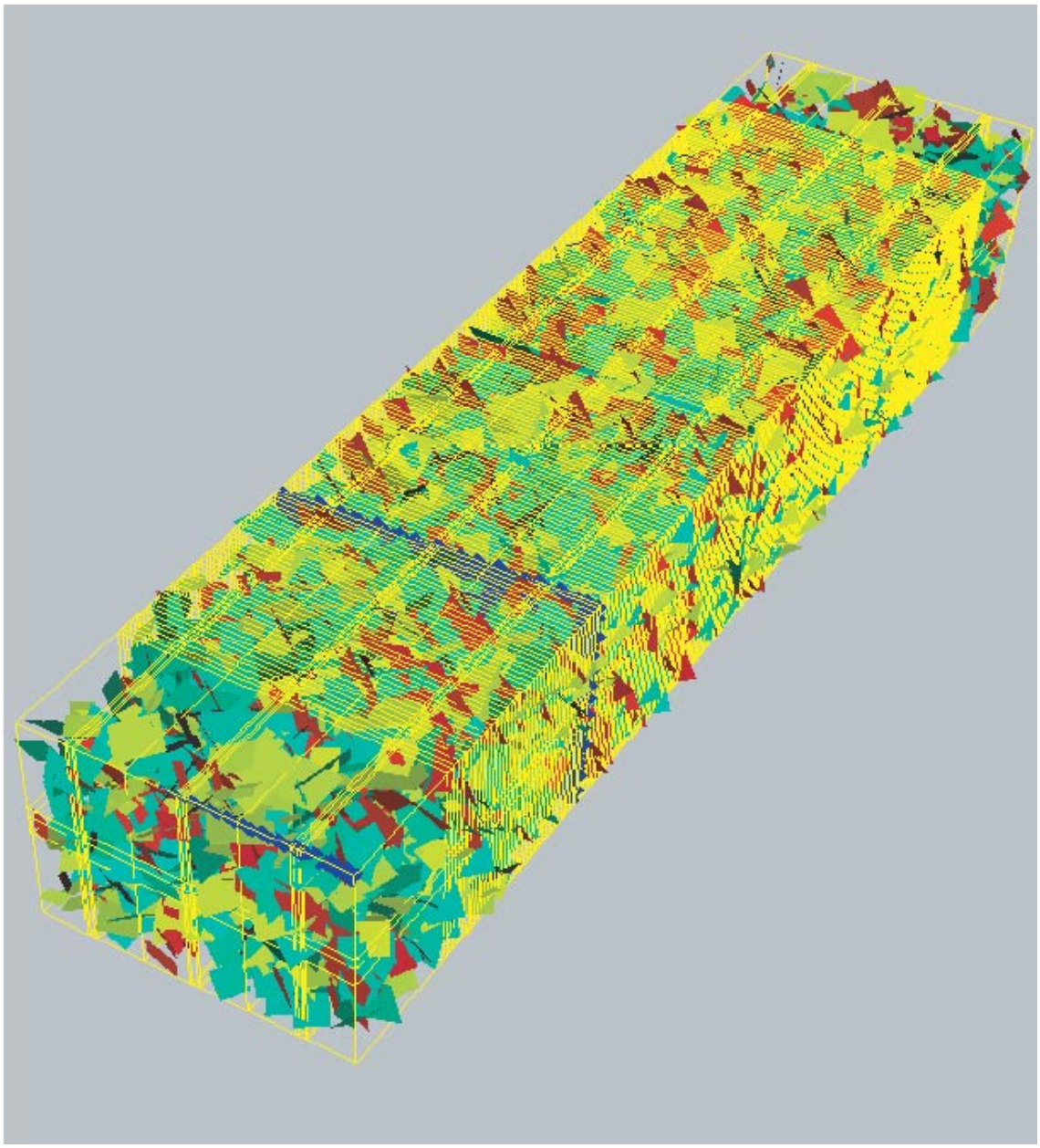

Figure 4-4. *Oblique view of the canister-scale model showing the fracture network. Here fractures are coloured by set. The random fractures are red, green and cyan. The low conductivity Zone 10W cuts through the model as represented by a tessellated (sub-divided) plane coloured dark blue.*

Figure 4-5 shows the tunnels and fractures together by stripping away randomly 90% of the fractures. The full (100%) fracture network is dense so as to intersect with the canisters and tunnels on an average spacing around 5 m. Hence, there is scope for the engineered structures to provide extra continuity for flow through the fracture network, though the actual amount will depend on backfill and plug properties.

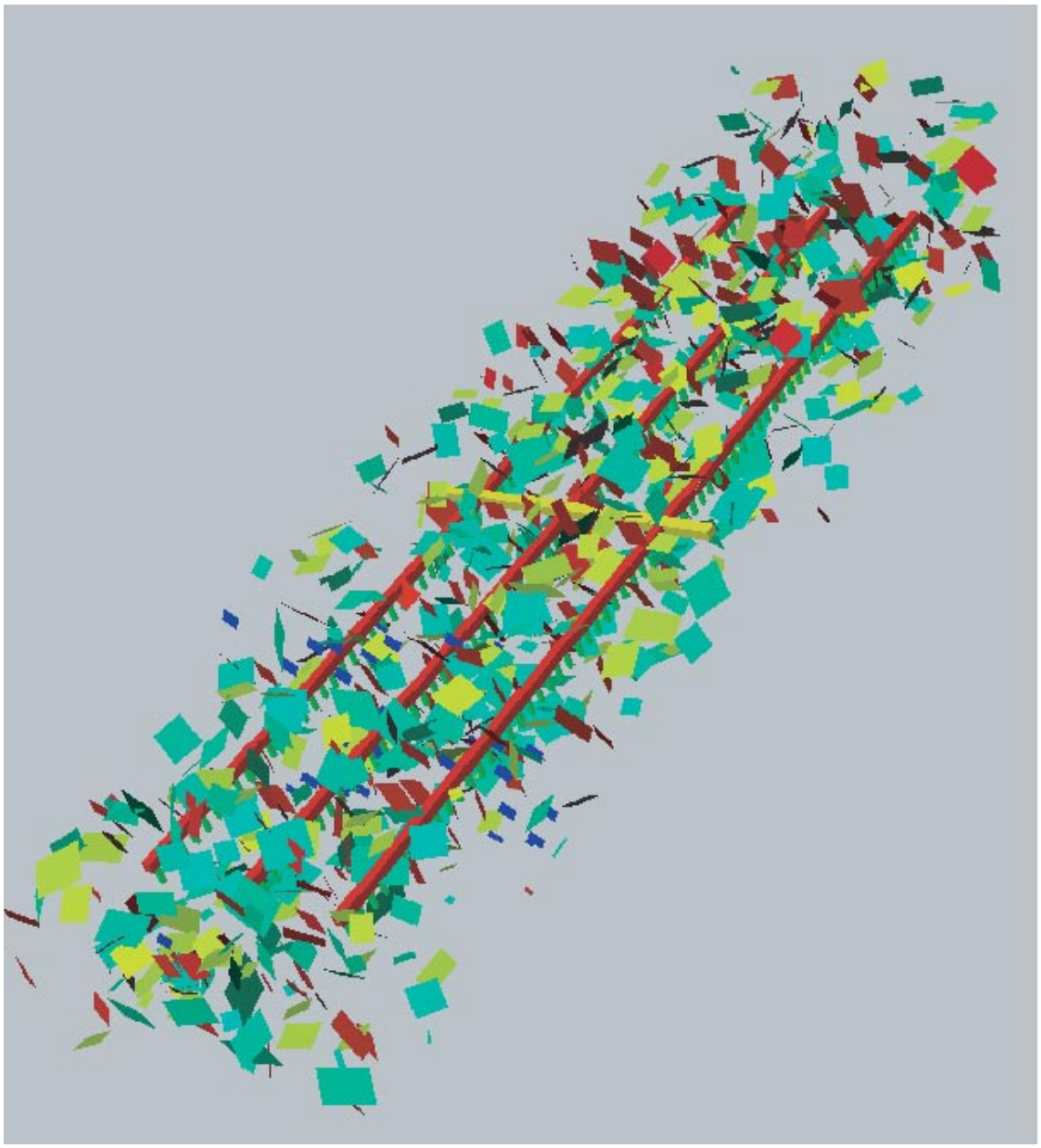

Figure 4-5. *The combined CPM model of the tunnels and deposition hole structure together with the DFN model of fractures. Only 10% of fractures are shown here, and fractures are coloured by set.*

4.1.1 Used data and assumptions

The geometry of the tunnel system is based on SR 97 Beberg data. The design for KBS-3 vertical was chosen. Hence, the distance between deposition tunnels is 40 m and the distance between deposition holes is 6.3 m. As an illustration and for test purposes a section of the tunnel system was modelled and located in the north-east corner of the northern rock block. That is, the canister-scale model with 6 tunnel sections and a section of roadway (see above) were located in the context of the Beberg repository design, and data from the Beberg structural model was used. As for the SR 97 calculations the depth for the tunnel system is 600 m.

As the technique to construct the tunnels has not been decided yet /Munier, 2002/, an assumption was made about the tunnel dimensions. The tunnels may be made by a full-face tunnel-boring machine or by a drill and blast technique. The choice of method may affect the extension and properties of the EDZ, Excavation Damaged Zone, /Rhén, 1998/.

Based on the design shown in Figure 4-6 a model is built in FEMGV, where the deposition holes were made about 8 m deep with a diameter of about 2 m. For simplicity a square cross-section was assumed rather than circular.

As an initial assumption, it may be assumed that the conductivity for the backfill material is as good as the rock mass. Also, it is assumed that the material in the deposition hole is compacted bentonite with a low conductivity. In this test a range of values were considered between 3 10^{-9} and 10^{-10} m/s. It may be a later task to calculate the impact of various design properties of the backfill and the material in the deposition hole. Table 4-1 shows the values of the permeability and porosity used for each of the parts of the CPM model.

The NAMMU part of the model contains approximately 2,000 elements and 5,500 nodes. The NAPSAC part contains around 6,400 fractures and 40,000 freedoms. The model is located at values of z between –649.8 and –558.0 m and values of x between 15.87 and 16.28 km, with y varying between 95.69 km and 96.17 km, with an approximate total model volume of $5.58 \cdot 10^6$ m^3.

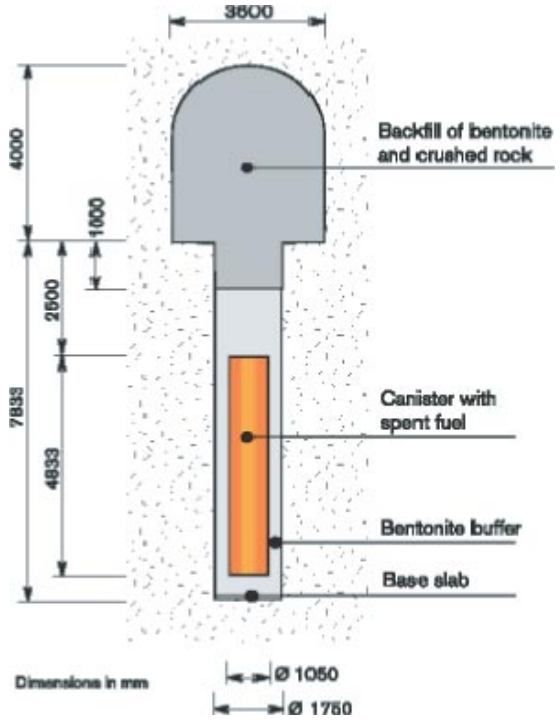

Figure 4-6. *Used design of deposition hole and tunnel.*

Table 4-1. Physical properties for different regions in the CPM model.

Material	K_{xx} (m^2)	K_{yy} (m^2)	K_{zz} (m^2)	Φ
Tunnels and access road	$3.26 \cdot 10^{-15}$	$3.26 \cdot 10^{-15}$	$3.26 \cdot 10^{-15}$	10^{-4}
Deposition hole	$3.00 \cdot 10^{-16}$	$3.00 \cdot 10^{-16}$	$3.00 \cdot 10^{-16}$	10^{-4}

Zone 10W cuts through the southern part of the tunnel with a low transmissivity of $1.08 \cdot 10^{-6}$ m^2/s. Zone 6W also just clips the upper southern edge of the model with a transmissivity of $9.63 \cdot 10^{-6}$ m^2/s. These zones are tessellated (subdivided) into 10 m sub-fractures to ensure a good discretisation. The random fractures have transmissivities varying between $1.1 \cdot 10^{-9}$ and $9.7 \cdot 10^{-5}$ m^2/s. As in Task 1, the details are taken from the Aberg model. The transmissivity is given by a truncated log-normal distribution of mean –15.62 and spread 1.86 (truncated between –20.7233 and –7.0). The length of the fractures is also distributed according to a log-normal distribution, with mean 2.373 and spread 0.472. The total number of fracture intersections is approximately 51,000. Figure 4-7 shows the fractures in the model coloured by transmissivity.

Boundary conditions needs to be specified in two places:

1. An internal boundary condition that links the pressure in the fractures to the pressure in the CPM model of tunnels and deposition holes. The purpose of this boundary condition is to ensure continuity of pressure and conservation of mass (flux) at the position where fractures intersect with the tunnels and deposition holes. If such a boundary condition is not specified in CONNECTFLOW then there is no flow at the interface between the two regions, which in this case would mean no flow in the tunnels or deposition holes.

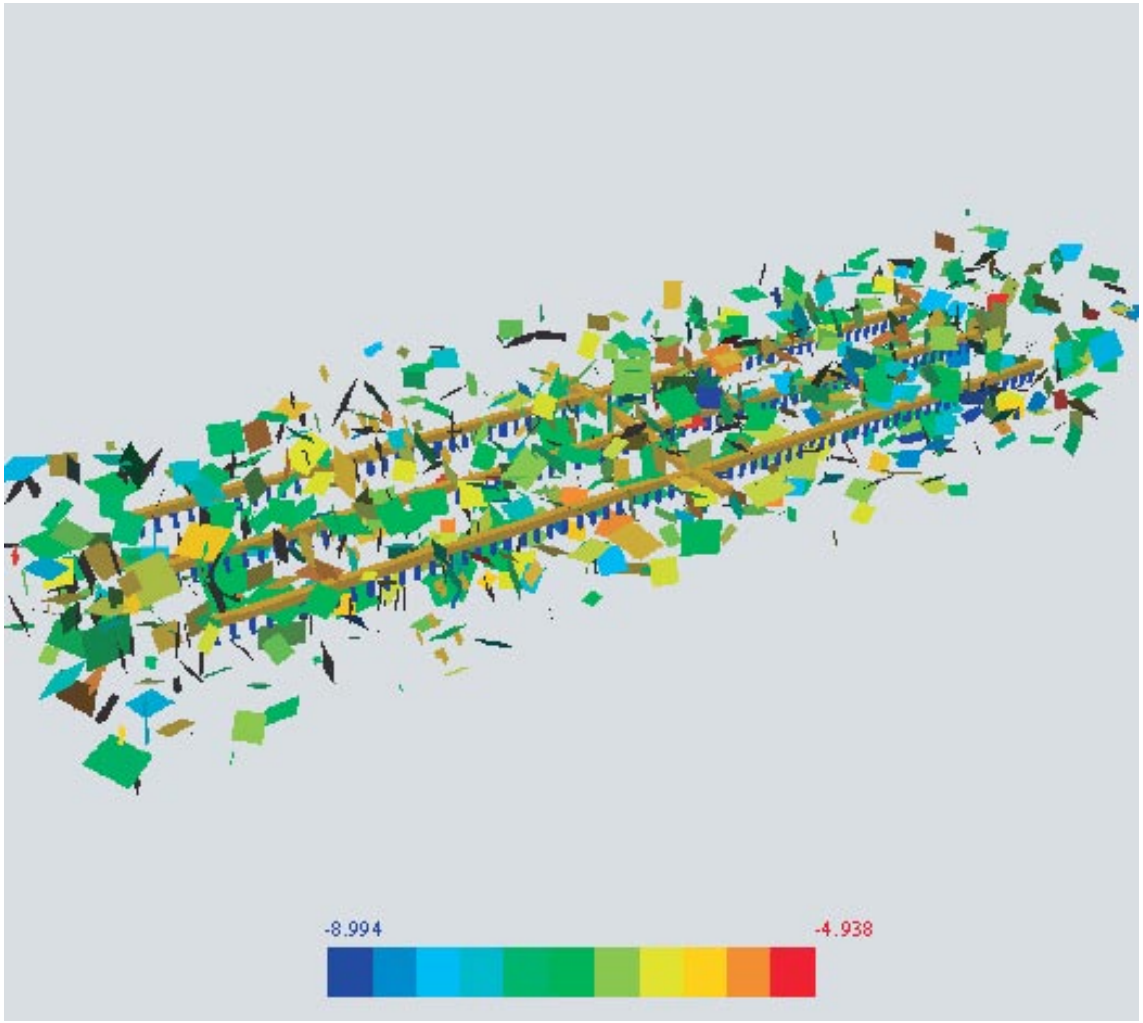

Figure 4-7. *Random fractures coloured by transmissivity and using a logarithmic scale. (10% of the fractures are shown in the figure).*

2. An external boundary condition to specify the insitu pressure distribution on the external boundaries of the DFN region. This boundary condition will control the overall pressure gradient and hence flow-rates through the local model.

The first condition is implemented by specifying a boundary condition on the internal surfaces of the DFN model that corresponds to the surfaces of the tunnels and deposition holes as represented by the CPM region. In terms of specifying the model, the user has to select the internal surfaces of DFN model and impose a coupling type of boundary condition. Surfaces are selected in CONNECTFLOW by obtaining the restricted list of surfaces that satisfy geometrical criteria. These criteria are of two forms: the corners of the surface have to either lie within coordinate limits (the coordinate system can be translated and rotated from the standard x, y, z), or the normal to the surface has to be close to that of a specified vector to within a given tolerance angle. In this way, different sets of surfaces can be selected relatively easily even for complex geometries by choice of appropriate coordinate limits, normal vectors and tolerance angles. Here, the internal surface was selected as all the surfaces within a cuboid that is slightly smaller than DFN model. The cuboid is defined by specifying axes rotated and translated to align with the model. Having specified a coupling boundary condition, CONNECTFLOW automatically identifies the fracture intersections with the internal boundaries of the DFN model, and then calculates which finite-elements these fractures intersect on the CFM side of the interface. Once it has been determined which fracture intersections connect to which finite-elements, then the equations are modified for these objects such that the pressure on the fracture intersection is an interpolate of that in the adjoining finite-element, and the flux that enters/exits the fracture intersection exits/enters the adjoining finite-element. Hence, in the interface condition a two-way coupling is used.

The second condition is specified as standard Dirichlet boundary conditions for pressure on the external boundary surfaces of the NAPSAC region (the outer surface in this case). The boundary conditions for the external surfaces of the model were obtained from a regional-scale CPM model based on that used in Task 1, but with the local-scale region all CPM rather than a nested DFN region. In this case, the local-scale CPM model had elements of about 35–40 m in size. The pressure values appropriate to the section of the repository considered here was then calculated for each planar surface of the model and saved to a file. On each surface the pressure distribution was saved on a grid of 2 m spacing. The pressure distribution on the external surfaces of the DFN model was then interpolated on to any fracture/boundary intersection. The resulting pressure distribution on the surface of the DFN model is shown in Figure 4-8. The range of head values for this region of the repository is 25.5 m to 27.7 m with the general trend going from southwest (high) to northeast (low). The head gradient is about $6 \cdot 10^{-3}$. It is expected that flow will be aligned approximately 10 degrees more east than the alignment of the tunnels. It should be noted that this section of the tunnels has been placed in the northeast corner of repository close to Zone 1 that runs parallel to the tunnels just to the east. This is evident in the low head gradients on the eastern side of the model. If the tunnel section were located in a different part of the repository the head gradients may be different. For example, if a section of tunnel was studied further west then the head gradient is more parallel to the tunnels. In terms of performing more detailed near-field studies, several sections of tunnels could be modelled by studying flows in different areas of the repository. This would be relatively easy. It would only require a different translation to the canister-scale mesh, and calculating the appropriate external boundary conditions for the new region from the regional-scale CPM model.

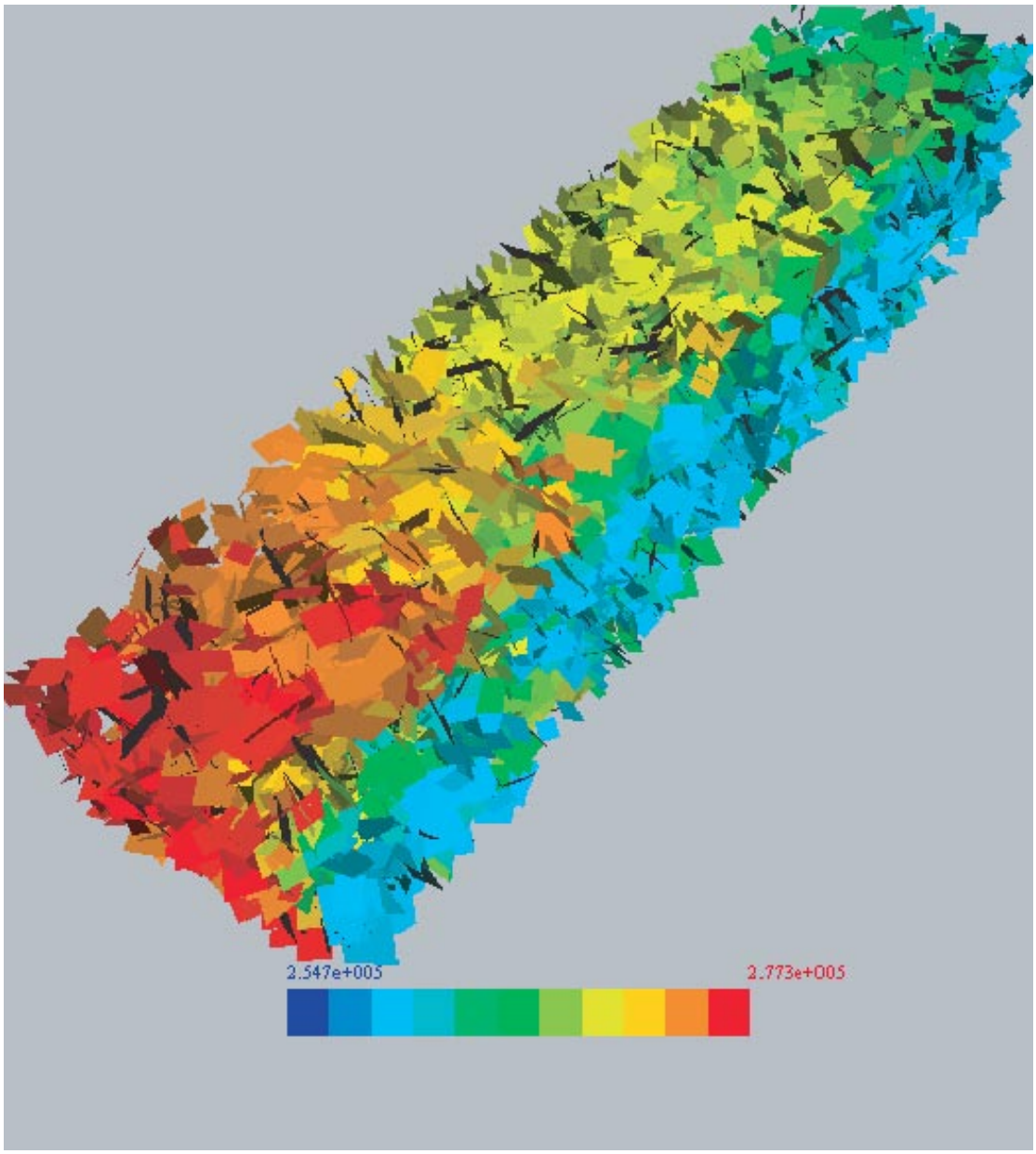

Figure 4-8. *The distribution of pressure interpolated from a regional-scale CPM model on to the external surface of the nested canister-scale model. Here the fractures in the DFN part of the model are coloured according to the average pressure varying between a maximum (red) of 27.7 m head and a minimum (blue) of 25.5 m head.*

4.2 Results

The system was solved using the GMRES preconditioned conjugate gradient method in about 600 s on a Dell Pentium 4 1.0 GHz processor.

The average head on the interface between the DFN and CPM parts is 26.7 m. The total flux from the NAPSAC to the NAMMU part of the model is approximately $2.96 \cdot 10^{-3}$ kg/s. The residual flux from a flux balance calculation is $6.6 \cdot 10^{-7}$ kg/s. The pressure solution for the combined model is shown in Figure 4-9. This demonstrates the consistency in pressure distribution between the CPM and DFN parts that ensures a match in both pressure and flux. In nesting a hydrogeological model of the engineered structures and fractures in this

way it is possible to study the interconnection of these systems and how they effect flow. For example, it is possible to study whether there is preferential flow along the tunnels and whether transverse flows re-enter the tunnels several times.

Figure 4-10 shows the distribution of Darcy velocities along the fracture planes. Only the fractures with a relatively high velocity (>10^{-8} m/s) are shown. This shows that large flows occur in only a few places, including Zone 10W and in the southeast corner of the model. Presumably this results from the steep head gradients in this corner due to the presence of Zone 1 just outside the model to the east.

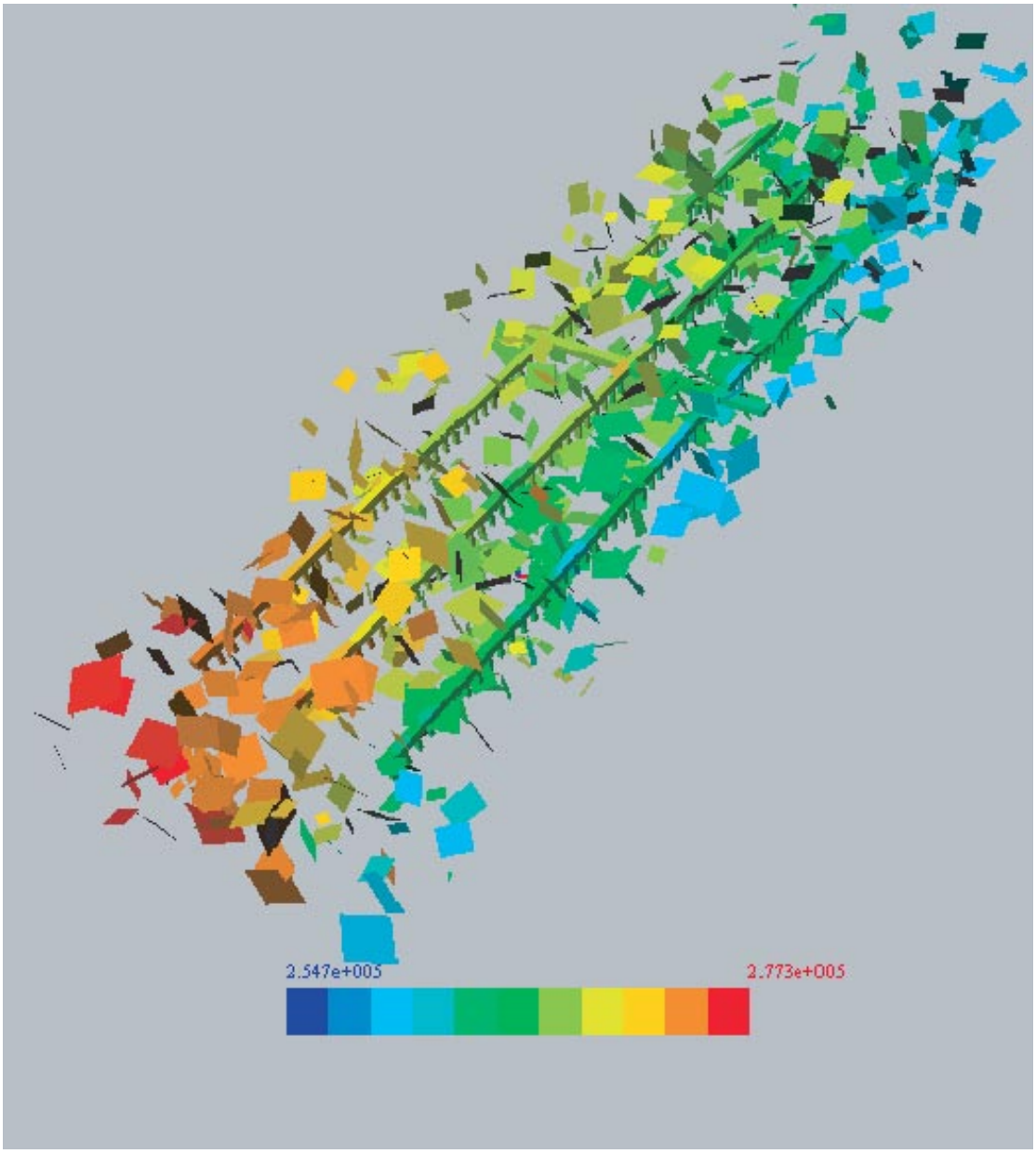

Figure 4-9. *Pressure distribution in the nested model with CPM model of tunnels and canisters together with fractures. The finite-elements and fractures are coloured by pressure on the same scale. Here, only 10% of fractures are shown to reveal the CPM model in the centre.*

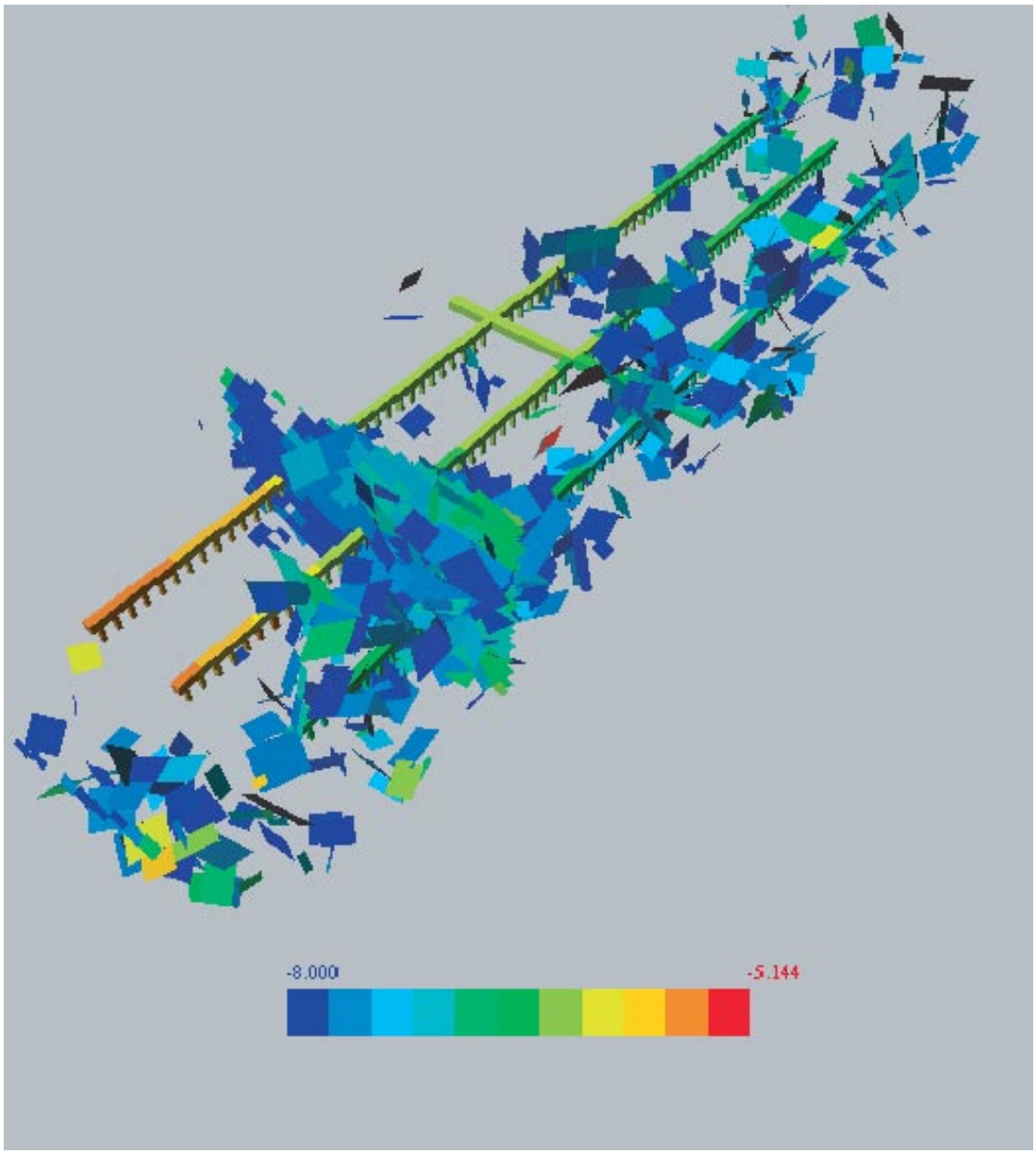

Figure 4-10. *Fractures coloured by the plane Darcy velocity using a logarithmic scale, with 10% of the fractures shown.*

Flows in the tunnels are shown in Figure 4-11 by drawing arrows aligned with local direction of flow in the CPM model. This shows that for sections of tunnels and roadways the flow follows the tunnels, but at regular intervals flow go through the tunnel walls into or out off the fracture network. The lower figure superimposes the fractures adjoining the tunnels and colours them by Darcy velocity to show how these flows enter the fracture system. The highest flow rates (green and red arrows) are in the eastern most tunnel which corresponds to the highest flows in the fractures. This shows how such models could be used to obtain more detailed and realistic statistics of flows in the engineered structures. Figure 4-12 shows 162 pathlines through the combined model starting in each canister. Generally pathlines move from west to east, although in the northeast the flow is more toward the north. This is consistent with the external boundary head gradient. Paths do not follow the tunnel for a significant distance, although there are cases where paths starting in the west enter either of the tunnels to the east at least for a short distance. Hence, there is a potential for contaminants from different canisters to interact.

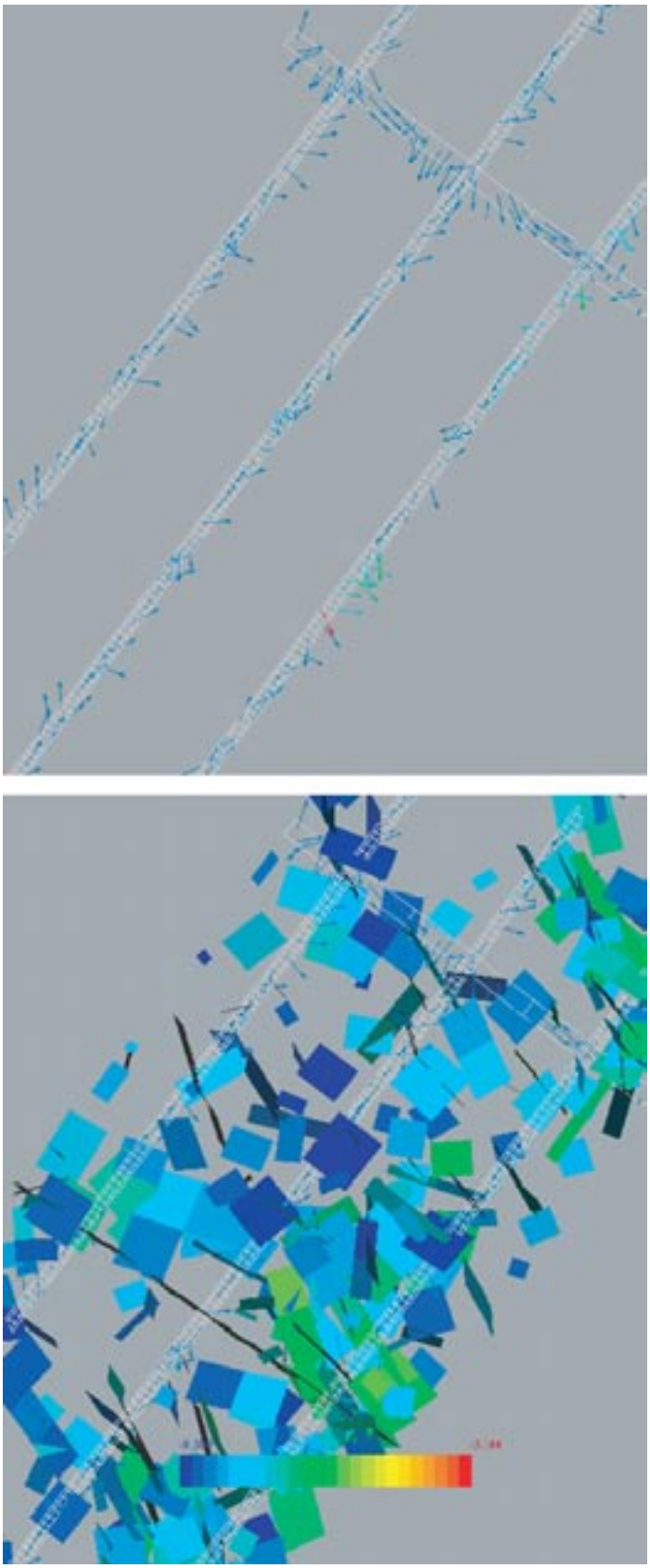

Figure 4-11. *Flow directions in the tunnels and roadway. Top: Velocity arrows in the CPM model only with orientation parallel to the local flow direction and coloured on a logarithmic scale according to the magnitude of velocity. Bottom: velocity arrows together with fractures at repository level coloured according to the logarithm of average Darcy velocity. Only fractures with high velocities are shown.*

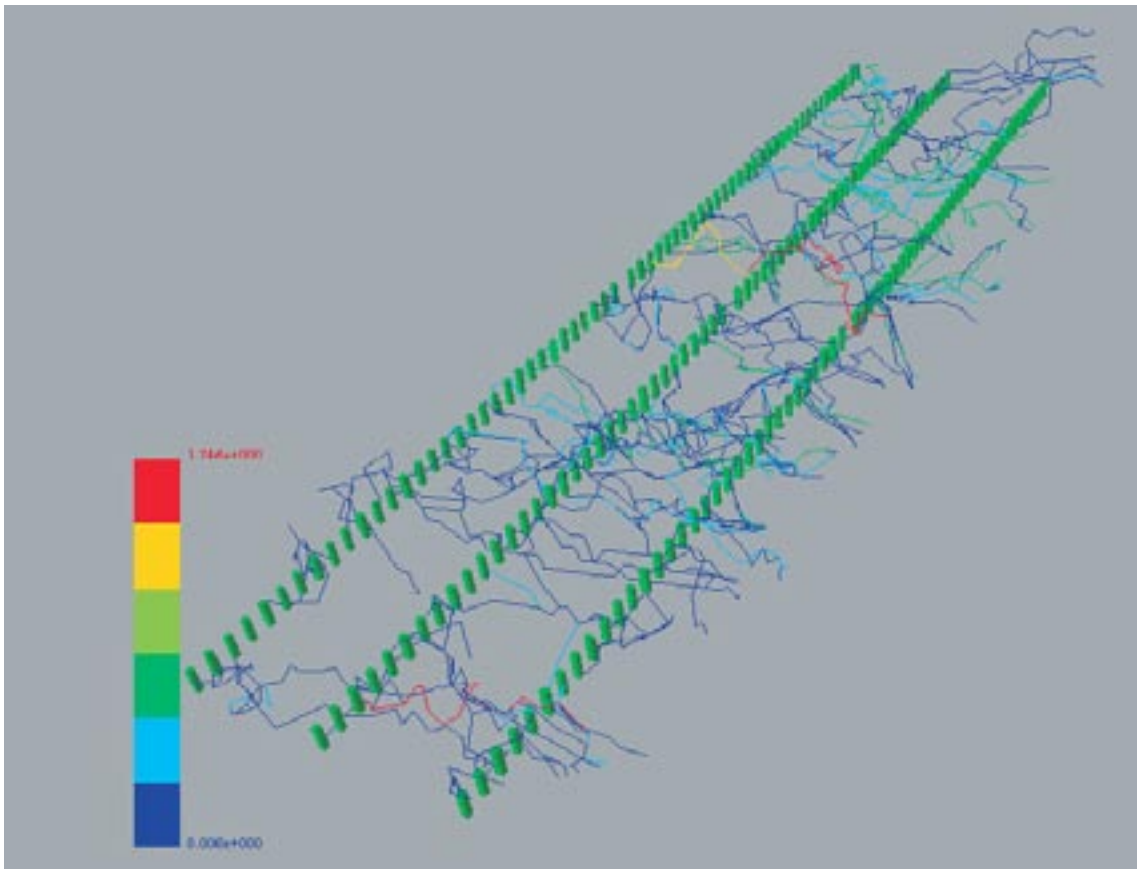

Figure 4-12. *Pathlines through the combined DFN/CPM model starting at each of the canister locations. The pathlines are coloured according to logarithmic time between 0 and 17.5 years. Pathlines generally exit the model on the eastern boundary.*

4.3 Task 3 implications

The preliminary tests in Task 3 are promising for enhancing the resolution in the characterisation of groundwater flow around engineered structures, and in particular for supplying realistic input to a near-field model. It may also be suitable to study statistics of e.g. the frequency of fractures intersecting tunnels and fractures intersecting deposition holes. This kind of calculation depends on purely geometrical data of fracture frequency. However, by studying the flow characteristics on the canister-scale useful information may be obtained on design issues, such giving an estimate on how many deposition holes may have to be abandoned due to high flow rates above a given criterion e.g. a certain level of conductivity or a level of influx. The flow-rate is not only a function of conductivity and gradient, but also the fracture connectivity. A too high flow rate through the deposition hole wall is not solely critical in case of canister failure, but also may cause difficulties when the compacted bentonite is to be inserted.

The CONNECTFLOW concept might also be used to study the impact of the properties of the tunnel back-filling material and the outcome of an incompletely filled tunnel. The choice of tunnel construction technique might also be studied by including the properties of the Engineered Damage Zone (EDZ) in the tunnels. Other design issues might also be addressed e.g. the possible improvements of using plugs in the tunnels.

One advantage in CONNECTFLOW is that it is flexible in the sense that it is easy to modify a domain from being CPM to DFN and vice versa. For example, if a region is modelled as CPM in the vicinity of the tunnel it may easily be altered to DFN. It is also possible to nest a CPM model within another CPM model. The inner model may then have a finer discretisation than the outer model to obtain higher resolution results near e.g. a repository. This has been demonstrated by /Marsic et al, 2001/.

4.4 Development work within Task 3

Development work was required to handle the coupling of the fractures to the CPM elements for the interface boundary conditions. Prior to this development it was only possible to select the surfaces where an interface condition was required by selecting patch faces one at a time. In this case, the geometry was complex in two ways: the internal interface was made up of 5,428 quadrilaterals and the mesh had been rotated to align with the tunnel orientation at Beberg. To solve this problem a new way of specifying the location of boundary conditions was implemented. This is done by specifying a set of vectors that define a rotated coordinate system, and then the list of surfaces is calculated that match a set of criteria based on whether nodes on the surface are within specified coordinate limits and whether the normal to the surface is aligned with a specified vector to within a specified tolerance angle. This approach offers much flexibility in defining boundary conditions for complex meshes.

To test the concept under realistic boundary conditions it was not desired to impose a realistic pressure distribution on the external model surfaces. This was done so that flow and pathline calculation may be performed using outer boundary conditions from Beberg regional model. One aim is to obtain the flow rate distribution in the vicinity of the repository on a detailed scale and another is to study pathlines from the deposition holes. The effect of using detailed input data in a near-field model may be illustrated. In addition, design issues related to the tunnel construction may be addressed. The practical limits of the concept may also be tested.

5 Application of the repository-scale model

In Task 4, the CONNECTFLOW concept is used to calculate more realistic input to a near-field model since it models explicitly the flow in the fracture system around the canisters together with the exchange of flow between the natural fracture system and the backfilled tunnels and deposition holes. It is proposed that this more geologically realistic concept be used to assess the validity of current assumptions made in near-field models and the derivation of the flow parameters used as input to these models.

Traditionally, the near-field model considers different flow paths, e.g. fractures directly connected to the deposition hole, the disturbed zone, the backfill or disturbed zone and then into a fracture zone connected to the tunnel, and transport by diffusion and then into an adjacent fracture. This concept is shown in Figure 5-1. In previous assessments these flow paths have been quantified based in CPM models. However such models give specific flow rates based on scales large relative to the canister-scale, and so factors have to be used, but a loss in resolution and accuracy is likely to result. Important questions arise regarding this methodology, such as whether the current assumptions are overly conservative, or are there cases where the greater heterogeneity inherent in DFN models gives rise to occasional very high flows that impact on the near-field in a significant way. Here these issues are addressed by using a CONNECTFLOW concept to provide input to near-field models. The model described in Task 3 is used for this purpose as it includes a more appropriate level of detail required to quantify issues of flow around canister locations and in the adjacent engineered structures.

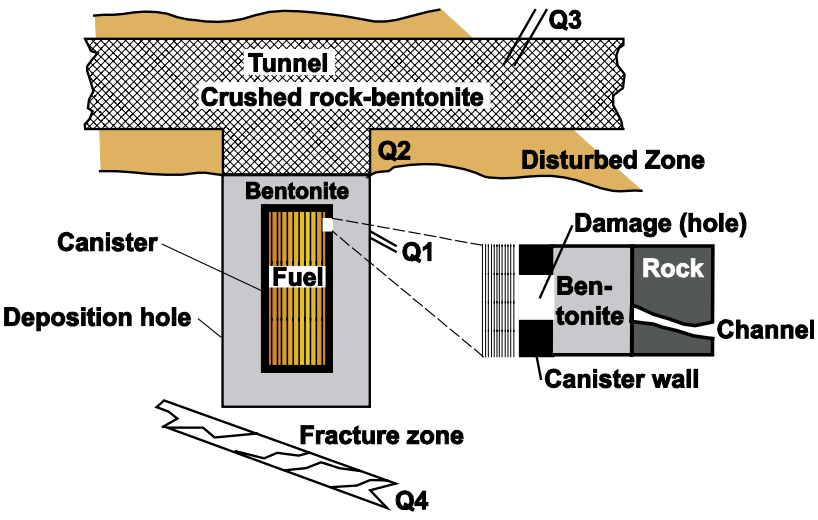

Figure 5-1. *Conceptual view of the release paths in the near-field model COMP23.*

In the potential case of a small hole in the canister wall, dissolved radionuclides may leak out, diffuse into the bentonite clay and may then migrate through various pathways into the flowing water in rock fractures. Figure 5-1 shows four possible pathways from a canister/deposition hole:

- Q_1: Into a fracture intersecting the deposition hole, the fracture is located adjacent to the damage on the canister wall
- Q_2: Into a fractured section around the upper part of the deposition hole, the Excavation Disturbed Zone (EDZ) around the deposition tunnel
- Q_3: Into the backfill in the tunnel and further to a large fracture (or small zone) intersecting the deposition tunnel
- Q_4: Into a nearby fracture or fracture zone located below the deposition hole with "good rock" between.

The intersection between the fracture/fractures and the deposition hole and between a fracture/fracture zone and the deposition tunnel may cover the whole circumference or only a fraction of the circumference. From sensitivity studies by /Romero et al. 1996/, it is found that the Q_1 and Q_2 pathways dominate for almost any choice of Q_3 and Q_4. Thus, in this study we have considered the two crucial pathways Q_1 and Q_2 only.

5.1 Background

SKB is using NUCTRAN /Romero, 1995/ to calculate transport of radionuclides from a possible defective canister into the far field. NUCTRAN is included in the Performance Assessment model chain PROPER that calculates the release from the canister into the biosphere. In the chain, NUCTRAN is denoted COMP23. In order to calculate the transport of radionuclides by diffusion into the flowing water in the rock, NUCTRAN uses the concept of equivalent flow rate, Q_{eq}.

For compartments in contact with water flowing in fractures in the rock, the diffusive transport is determined by an equivalent flow rate Q_{eq}. This parameter is a fictitious flow rate of water that carries a concentration equal to that at the compartment interface. It has been derived by solving the equations for diffusional transport to the passing water by using boundary layer theory /Neretnieks, 1979/. The value of Q_{eq} is dependent on the geometry of the contact area, the water flux, the flow porosity and the diffusivity. To illustrate the entities used in the definition of the equivalent flow rate, the water flow in the rock surrounding the deposition hole is shown in Figure 5-2. The Darcy velocity in the rock around the deposition hole is denoted U_0. The length of the water path is L. W in Equation 1 below is used to calculate the interface area for diffusion and is equal to the height of the canister. In this case, since the water flows around both sides of the canister, 2W is used in the calculations.

To define the equivalent flow rate the following equation is used /Romero, 1995/:

$$Q_{eq} = 2 \cdot W \cdot U_0 \cdot \bar{\eta} = 2 \cdot W \cdot U_0 \cdot \sqrt{\frac{4 \cdot D_w \cdot t_w}{\pi}} \qquad (1)$$

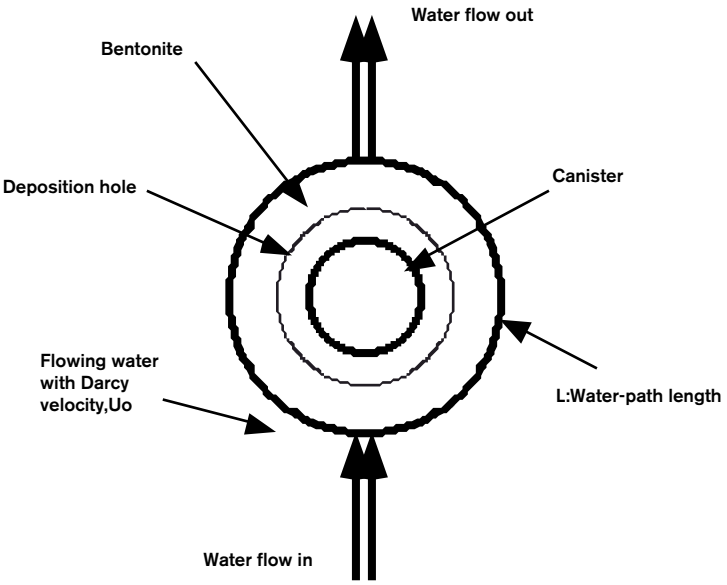

Figure 5-2. *Schematic view of the water flow around the rock surrounding the deposition hole.*

The contact time with the flowing water is determined from the Darcy velocity U_0, the flow porosity ε_f, and the length of the pathway L in contact with the flowing water:

$$t_w = \frac{L \cdot \varepsilon_f}{U_o} \qquad (2)$$

where:

U_0 is the Darcy velocity (water flux) [m^3/m^2/year],

W is a geometric parameter used for the width of the surface area in contact with the flowing water in fractures, fracture zones, or EDZ, [m],

$\bar{\eta}$ is the mean thickness of the penetration in the fracture by diffusion from the compartment, [m],

D_w is the diffusivity in water, [m^2/year],

t_w is the time the water is in contact with the compartment, [year],

L is the length of the pathway in contact with the flowing water, [m], and

ε_f is the flow porosity, [–].

5.2 Approach

Here these issues are addressed by using a CONNECTFLOW concept to provide input to near-field models. The CONNECTFLOW model described in Task 3 is used for this purpose as it includes a more appropriate level of detail required to quantify issues of flow around canister locations and in the adjacent engineered structures. To communicate this more accurate input to COMP23 a number of output facilities from CONNECTFLOW have been implemented and tested. This is done by calculating gross flow-rates adjacent to each of the canisters and nearby tunnel. The flows are then written to an ASCII formatted file for statistical processing. For path Q1, fluxes in all fractures intersecting each canister are calculated. Ideally, one $Q_{eq,1}$ value for each fracture should be calculated and e.g. the resulting $Q_{eq,1}$ value for that deposition hole can then be exported to the near-field calculation tool.

The method of deriving Q2 has more possibilities and here the key issue is how to represent the disturbed zone around the tunnel. For example, the distribution of flux out of small fractures that intersect the tunnel could be derived and used as a distribution independent of the canister flux Q1. The problem is to choose which fractures that best represent the Excavation Damaged Zone, EDZ, near the deposition hole. The EDZ may also be modelled as a planar fracture in parallel to the tunnel. For this option this artificial fracture has to be based on e.g. flow rates or apertures of the small fractures it is representing. A third option is to represent the EDZ with a porous media layer around the tunnel. Alternatively, the flux through the continuum section of the tunnel immediately above each deposition hole could be used as an approximation in this project. The latter method is used here to illustrate that we can obtain flow rates in the tunnel and the kinds of results that are obtained.

Having developed the output facilities and concept for Q1 and Q2, the statistics of Q1 and Q2 are derived for a nested CONNECTFLOW model and compared to an equivalent stochastic continuum model to illustrate how the input to COMP23 compare for the two flow models. Here some simple distributions/histograms are generated to quantify measures such as: how many fractures are cut by each canister, and what are the canister fluxes, travel times and F-quotients for paths. The aim is to produce such measures to aid discussions on how this more complex data might be represented by near-field models in an appropriate methodology.

By using the model in Task 3 and starting the pathlines in the deposition holes results are obtained such as the number of fractures that intersect the deposition hole and the total flow rates in these fractures. For path Q1, fluxes in all fractures intersecting each canister can be calculated. This type of information is then used to calculate Q1. The method of deriving Q2 is to calculate the flux through the continuum section of tunnel immediately above each deposition hole. Here, Q2-values are calculated by starting the pathlines in the tunnel just above the deposition hole.

A reference case is also calculated based on a pure CPM model using the same boundary conditions and starting positions as the Task 3 model. The reference case is used for comparison with the values using the Task 4 approach.

5.3 Results

As mentioned, Task 4 results are obtained from a model built on Task 3. Hence, the model consists of a CPM domain within a DFN domain. In summary, the model contains 192 deposition holes distributed on six tunnel segments. The tunnel segments including the deposition holes and an access tunnel are built as a continuous porous medium. Around the tunnels a stochastic fracture network is created. The boundary conditions are calculated in a regional CPM model.

The number of fractures intersecting each deposition hole is recorded as well as the flow rates in these fractures. Ideally, one $Q_{eq,1}$ value for each fracture should be calculated and e.g. the resulting $Q_{eq,1}$ value for that deposition hole can then be exported to the near-field calculation tool COMP23. For this demonstration and practical reasons, the sum of the flow rates in the fractures intersecting a deposition hole was used to calculate the equivalent flow rate $Q_{eq,1}$. In future calculations, it is recommended that $Q_{eq,1}$ is calculated for each fracture intersecting the deposition hole and e.g. the resulting $Q_{eq,1}$ is reported. The distribution of the number of fractures that intersect deposition holes are shown in Table 5-1 and Figure 5-3.

Table 5-1. Distribution of deposition holes intersected by a particular number of fractures.

Number of intersections	0	1	2	3	4	5
Percentage, %	17.2	31.8	29.7	16.1	4.7	0.5

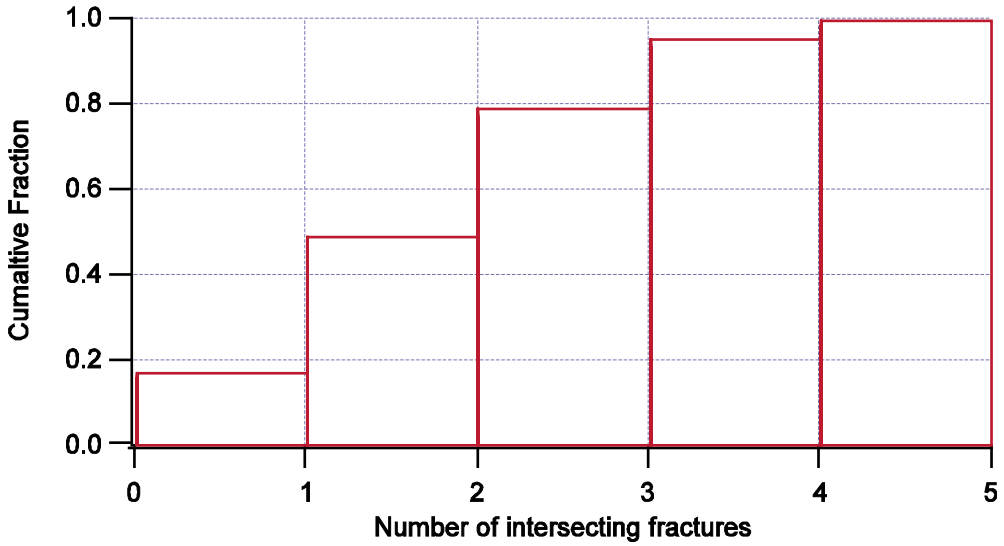

Figure 5-3. *Cumulative distribution of deposition holes intersected by a particular number of fractures.*

Another difficulty is that the diffusivity, D_w, is radionuclide specific. Therefore, the values, here denoted as QEQ, exported from CONNECTFLOW do not include D_w. To obtain input to COMP23 the values from CONNECTFLOW should be multiplied by nuclide specific $\sqrt{D_w}$. Although the diffusivity of radionuclides differs, in SR 97 a single value of $D_w = 1\times10^{-9}$ m^2/s (3.15×10^{-2} m^2/year) was suggested as an approximation. Hence, the values from CONNECTFLOW is here multiplied by $\sqrt{D_w} = 0.178$ m/year$^{0.5}$ to enable comparisons. The distribution of $Q_{eq,1}$ values is shown in Figure 5-4. Hence, the equivalent flow rate in path Q1 may be imported to COMP23 as:

$$Q_{eq,1} = 0.178x\ QEQ$$

where QEQ [m^2/year$^{0.5}$] is the value obtained from CONNECTFLOW. Naturally, it would be better to use nuclide specific values.

5.3.1 Calculation of Q2

In the near-field concept, the potential transport path in the disturbed zone around the tunnel is denoted Q2. The magnitude of the disturbed zone, EDZ, may depend on the used excavation technique. In CONNECTFLOW there are many possibilities to represent EDZ. One option would be to calculate the flow rates in the small fractures intersecting the tunnel. Another option would be to represent all the small fractures with an artificial fracture, based on a suitable parameter to represent those small fractures, in parallel to the tunnel. A third option is to obtain the flow rates in a porous media layer around the elements representing the tunnel. In this project an approach is used which is similar to the third option, but since no elements are included representing the EDZ a simplification was made for demonstration

purposes. In this task, Q2 was calculated as the flux through the continuum section of tunnel immediately above each deposition hole. Here, Q2-values are calculated by starting the pathlines in the tunnel (that is represented by the CPM part of the model) just above the deposition hole. The equivalent flow rate in path Q2 is calculated as:

$$Q_{eq,2} = 2WU(4D_wL\varepsilon_f/U/\pi)^{0.5}$$

Where U is the flux at the starting position, W is used to define the contact area, L is the contact length, D_w is the diffusivity in water and ε_f is the flow porosity. It is assumed that the tunnel is constructed by a drill and blast technique. Hence, W is 2 m as in the estimations by /Moreno and Gylling, 1998/. L is half the perimeter i.e. 3 m in this case. The flow porosity is 10^{-4} and $D_w = 0.0315$ m^2/year. The results are shown in Figure 5-4.

5.3.2 Reference case, a CPM model

To be able to compare the Task 4 results, a pure CPM model was created as a reference case. The same 192 starting positions as in the Task 4 model were used. The boundary conditions are derived from the same regional model. In the Task 4 model it is possible to obtain actual flow rate values in the fractures intersecting the deposition holes. In the pure CPM set-up for comparison the flow rates need to be estimated since the resolution is much less. The approach is as the one suggested by /Moreno and Gylling, 1998/ in SR 97. In the first step the resulting flux at the starting position is calculated as:

$$U = (U_x^2 + U_y^2 + U_z^2)^{0.5}$$

In the second step the equivalent flow rate for the path Q1 is calculated as:

$$Q_{eq,1} = 0.03U^{0.5}$$

The results for the full CPM model in the reference case are shown in Figure 5-5. The values are calculated by using the equations above.

5.3.3 Estimation of Q2 in a CPM model

In the CPM reference case the equivalent flow rates need to be estimated since the resolution is much less. The approach is as the one suggested by /Moreno and Gylling, 1998/ in SR 97. Here it is assumed that the tunnel is constructed by a drill and blast technique. In the first step the resulting flux at the starting position is calculated as above. In the second step the equivalent flow rate for the path Q2 is calculated as below and the obtained values are shown in Figure 5-4:

$$Q_{eq,2} = 0.1U^{0.5}$$

5.3.4 Comparison of results

As may be seen the two distributions are totally different both in shape and values. In the Task 4 model about 17% of the deposition holes are not intersected by fractures. However, a large spread in values may be seen in the deposition holes that are intersected by fractures. A fraction of the deposition holes are intersected with high flow rates. The simulation results suggest that the median value is near –2.8 on the log10 scale.

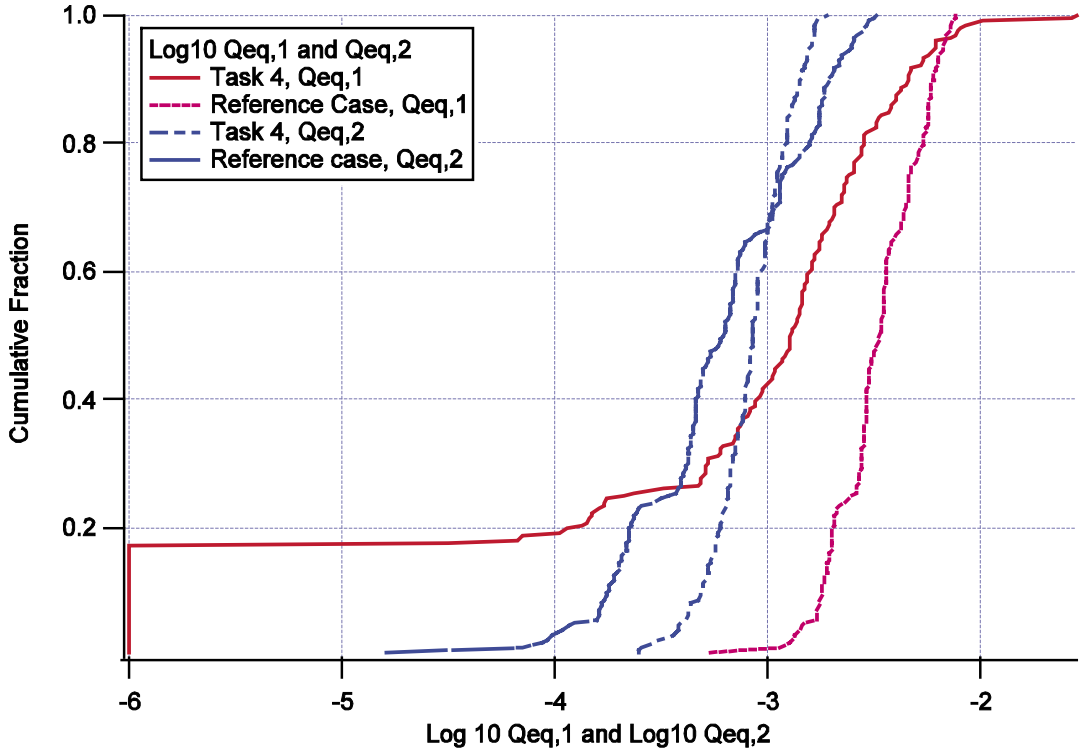

Figure 5-5. *Comparison of the results in Task 4 with estimations of Qeq,1 and Qeq,2 values from the Reference Case, i.e. a complete Continuous Porous Media model, CPM.*

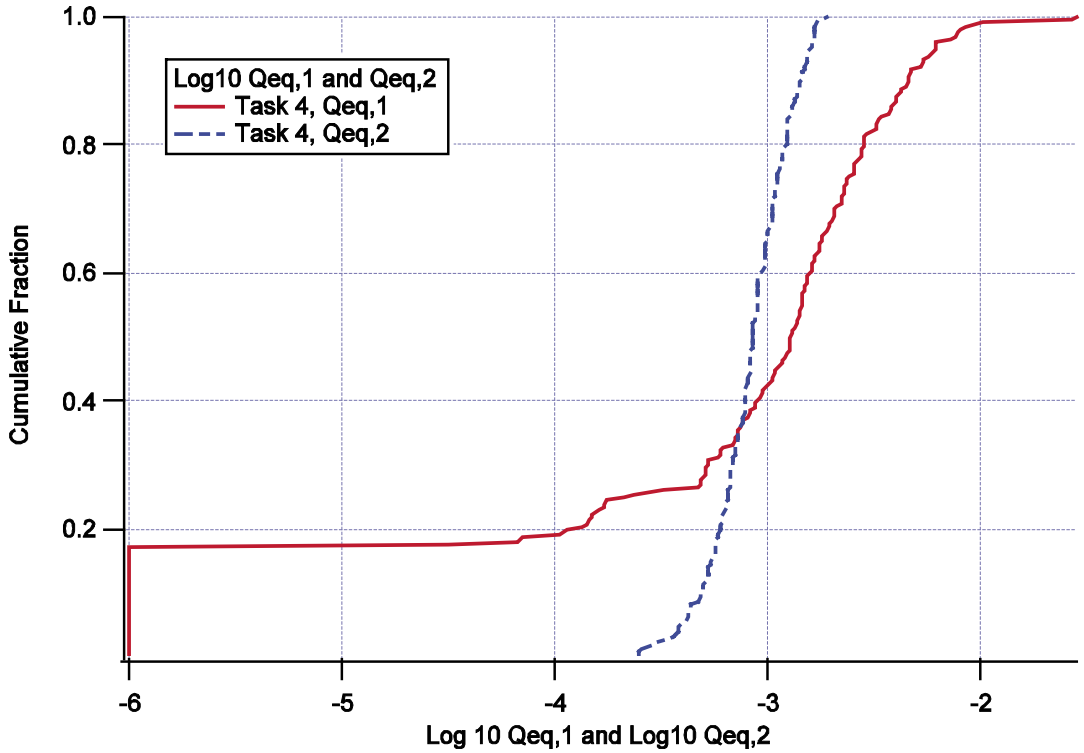

Figure 5-4. *Cumulative distribution of Log_{10} Qeq,1 and Log_{10} Qeq,2 values within Task 4. For deposition holes with no fractures intersecting the value –6 is arbitrary used.*

In the full CPM calculation, created for comparison, the distribution is more narrow and that the median value is around –2.5 on the log10-scale. One reason for the narrow distribution is that the CPM model is using a lower resolution in comparison to the nested model.

The statistical material is probably too small (too few values) to establish any firm conclusions. However, having this in mind, Table 5-2 is created as a simplified comparison of Q1 values. Also, bear in mind that only values for deposition holes intersected by fractures are included for the Task 4 model, whereas the reference case, i.e. the CPM model, all deposition holes are included.

In Table 5-3 a simplified comparison of Q2 values is given. Again, only 192 values are used in the comparison between Task 4 and the reference case. Differences in the distributions may be seen. However, some resemblance in the values may be seen.

Table 5-2. Simplified comparison of Log_{10} $Q_{eq,1}$-values from the Task 4 model with values estimated from the reference case, a pure CPM. The number of starting positions is 192.

Statistics	**Task 4, Q1, intersected holes only**	**Ref. CPM,** Q1
Average	–2.85	–2.49
St dev	0.49	0.21
Variance	0.24	0.04
Median	–2.82	–2.48
Min	–4.51	–3.27
Max	–1.56	–2.12

Table 5-3. Simplified comparison of Log_{10} $Q_{eq,2}$-values from the Task 4 model with values estimated from the reference case, a complete CPM. The number of starting positions is 192.

Statistics	**Task 4, Q2**	**Ref. CPM,** Q2
Average	–3.08	–3.23
St dev	0.18	0.41
Variance	0.03	0.17
Median	–3.07	–3.21
Min	–3.61	–4.79
Max	–2.72	–2.49

6 Summary

Models for Task 1, 2, 3 and 4 have been constructed. In all cases nested models have been created using CONNECTFLOW. One advantage to directly nest the models is that a better transfer of boundary conditions from one region to another is obtained compared to indirectly applying Dirichlet pressure boundary conditions only, between a regional model to a local-scale model, for example. A better flow balance is then ensured. Another advantage is the flexibility of changing a domain from DFN to CPM representation, or vise versa, easily and self-consistently. The workflow from data to model has been tested and is recorded here. The models and methods may be used as a platform for later studies.

Task 1 and 2 consider the case of a repository-scale DFN model nested within an embedded CPM model that includes both the site-scale and regional-scales. Task 1 demonstrates how such models can be constructed. Task 2 shows what results can be obtained using such a model by applying the model to Beberg and comparing the results for canister flux and transport statistics with results from pure CPM models as used in SR 97.

Since generic data was used for the DFN section the transmissivity distribution for the random fractures was modified to match the permeability statistics of the CPM domain. There is a feature in NAPSAC that was used to study equivalent block values. The resulting model contains a stochastic permeability field, constraints, topographic boundary condition and a DFN domain with inferred fracture zones and random fractures. The system was solved for pressure, flow and pathlines.

In Task 2, several realisations of the model were performed and analysed to obtain statistics of repository performance measures such as groundwater travel time and flux at starting positions. The results show good consistency in the mean values when compared to the HYDRASTAR modelling in SR 97 /Gylling et al. 1999/, but the variance is increased in the new nested model. This is to be expected since a DFN model offers much greater resolution in local-scale variability since it represents individual fractures on a few metres scale rather than the CPM approach where flows are effectively averaged out over a larger volume (e.g. 35 m cuboid elements). The inner flow balance between the CPM and DFN domains was studied with good results. The canister location process is addressed indirectly by examining how many deposition holes that may have to be moved if an assumed threshold is exceeded. Not surprisingly, some pathlines starting from positions near fracture zones have higher flows and shorter travel times to the surface compared to the ensemble mean.

Task 2 gave also an opportunity to test the recently developed method to calculate F-quotients directly in CONNECTFLOW. In the DFN domain F-values are calculated with good knowledge of the fracture area and flow rate. However, in the CPM domain the flow-wetted surface area has to be assigned to each rock type and fracture zone. Still, this is an improvement compared to the method used in SR 97.

The converse was done in Task 3 where a rather complex CPM model was nested within a DFN model. The CPM model represents a tunnel system with an access tunnel, deposition tunnels and deposition holes. A generic DFN model serves as framework and makes it possible to study fracture and repository intersections. The goal is to obtain detailed near-field flow rates and possibility to address design issues.

Traditionally, the near field model considers different flow paths, e.g. fractures directly connected to the deposition hole, the disturbed zone, the backfill or disturbed zone and then into a fracture zone connected to the tunnel, and transport by diffusion and then into

an adjacent fracture. By using specific flow rates from continuum models on scales large relative to the canister-scale, and applying factors, a loss in resolution and accuracy is likely to result.

In Task 4, the CONNECTFLOW concept is used to calculate more realistic input to a near-field model since it models explicitly the flow in the fracture system around the canisters together with the exchange of flow between the natural fracture system and the backfilled tunnels and deposition holes. It is proposed that this more geologically realistic concept be used to assess the validity of current assumptions made in near-field models and the derivation of the flow parameters used as input to these models. The CONNECTFLOW model described in Task 3 is used for this purpose as it includes a more appropriate level of detail required to quantify issues of flow around canister locations and in the adjacent engineered structures.

Distributions of Q1 and Q2 values are calculated. For calculations of Q1, flow rates in the fractures intersecting the deposition holes are used. For calculations of Q2, initial flux values in the tunnel just above the deposition holes are used. Other options to obtain Q2 values are possible. The calculated values in Task 4 are compared with a reference case using a CPM domain solely. A methodology, originally proposed for SR 97, to overcome the coarse resolution in the CPM is used to estimate values. Some resemblance in the median values may be seen.

As another part of this project a new software tool for presentation of statistical results is developed. The new tool is based on Matlab and denoted @STAT. The simulations in this project gave an opportunity to test this new tool.

Acknowledgements

The authors of this report would like to acknowledge the support, comments and guidance from Jan-Olof Selroos of the Swedish Nuclear Fuel and Waste Management Company (SKB).

We would also like to thank Luis Moreno at the Department of Chemical Engineering at the Royal Institute of Technology (KTH) in Stockholm, Sweden, for suggestions and comments related to the section on calculations of the equivalent flow rates.

Finally, we are grateful for the funding from SKB, which made this study possible.

References

Boghammar B, Grundfelt B, Hartley L J, 1997. Investigation of the large scale regional hydrogeological situation at Ceberg, SKB TR-97-21, Svensk Kärnbränslehantering AB.

Cliffe K A, Morris S T, Porter J D, 1998. Assessment Model Validity Document; NAMMU: A program for calculating groundwater flow and transport through porous media, SKB R-99-51, Svensk Kärnbränslehantering AB.

Dershowitz W, Eiben T, Follin S, Andersson A, 1999. SR 97 – Alternative models project, Discrete fracture network modelling for performance assessment of Aberg, SKB R-99-43, Svensk Kärnbränslehantering AB.

Gylling B, Walker D, Hartley L J, 1999. Site-scale groundwater flow modelling of Beberg, SKB TR-99-18, Svensk Kärnbränslehantering AB.

Hartley L, Boghammar B, Grundfelt B, 1998. Investigation of the large-scale regional hydrogeological situation at Beberg, SKB TR-98-24, Svensk Kärnbränslehantering AB.

Hartley L J, Holton D, Hoch A R, 2002. NAPSAC (release 4.3), Technical summary document, SERCO/ERRA-N/TSD02v1.

Hartley L J, Holton D, 2003. CONNECTFLOW (release 2.0), Technical summary document, SERCO/ERRA-C/TSD02v1.

Holton D, Milický M, 1997. Simulating the LPT2 and Tunnel Drawdown Experiment at Äspö using a Coupled Continuum-Fracture Network approach, SKB ICR 97-05, Svensk Kärnbränslehantering AB.

Marsic N, Hartley L J, Jackson C P, Poole M, 2001. Development of Hydrogeological Modelling Tools Based on NAMMU, SKB R-01-49, Svensk Kärnbränslehantering AB.

Moreno L, Gylling B, 1998. Equivalent flow rate concept used in the near field transport model COMP23 – Proposed values for SR 97, SKB R-98-53, Svensk Kärnbränslehantering AB.

Munier R, Sandstedt H, Niland L, 1997. Förslag till principiella utformningar av förvar enligt KBS-3 för Aberg, Beberg och Ceberg, SKB R 97-09, Svensk Kärnbränslehantering AB.

Munier R, 2002. Personal communication, Svensk Kärnbränslehantering AB.

Neretnieks I, 1979. Transport Mechanism and Rates of Transport of Radionuclides in the Geosphere as Related to the Swedish KBS-Concept, Proc. Symp. Underground Disposal of Radioactive Wastes, Otaniemi, Finland, July 2–6, 1979, Vol II. p 108, International Atomic Energy Agency, 1979.

Poteri A, 1996. Analysis of bedrock fracturing at Äspö, SKB ICR 96-01, Svensk Kärnbränslehantering AB.

Rhén I, 1998. EDZ – Förslag på konceptuell modell för säkerhetsanalys, SKB Arbetsrapport U-98-03, Svensk Kärnbränslehantering AB.

Romero L, 1995. The Near-field Transport in a Repository for High-Level Nuclear Waste. Ph.D. Thesis, TRITA-KET R21, 1995.

Romero L, Moreno L, Neretnieks I, 1996. Sensitivity of the radionuclide release from a repository to the variability of materials and other properties, Nuclear Technology, 113 (3), 316–326, 1996.

Serco Assurance, 2004. www.connectflow.com.

Selroos J-O, Walker D, Ström A, Gylling B, Follin S, 2002. Comparison of alternative modelling approaches for flow and transport in fractured rock. Journal of Hydrology, 257, 174–188.

Walker D, Rhen I, Gurban I, 1997. Summary of hydrogeologic conditions at Aberg, Beberg and Ceberg, SKB TR 97-23, Svensk Kärnbränslehantering AB.

Walker D, Gylling B, 1999. Site-scale groundwater modelling of Ceberg, SKB TR-99-13, Svensk Kärnbränslehantering AB.

Walker D, Gylling B, Ström A, Selroos J-O, 2001. Hydrogeologic studies for nuclear-waste disposal in Sweden, Hydrogeology Journal, 9, pp 419–431.

Appendix A

Task 3

Figure A-1 shows the repository region for Beberg with identified fracture zones and rock volumes. Figure A-2 shows the repository layout for Beberg used in SR 97.

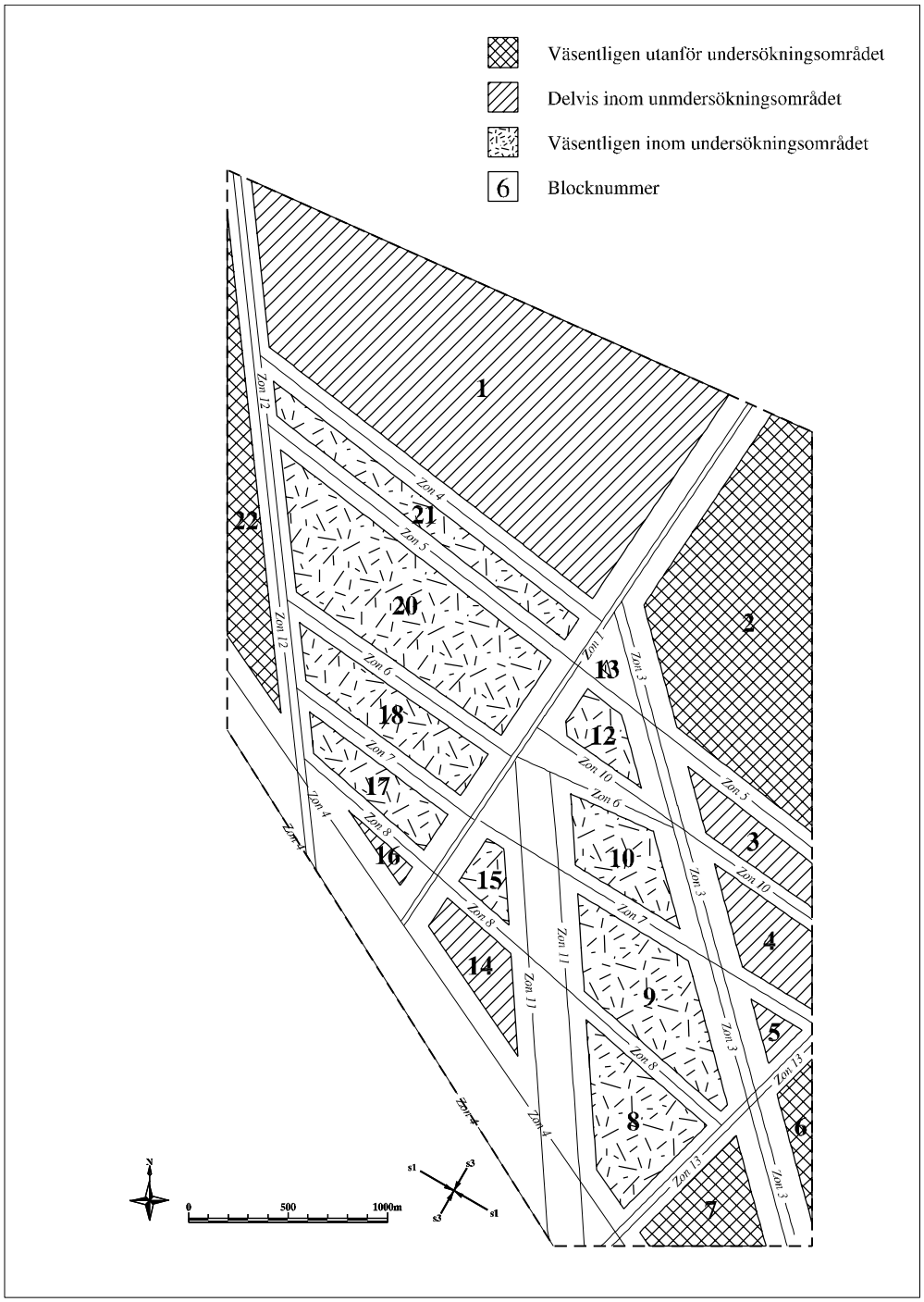

Figure A-1. *Repository region and rock volumes used for repository design at Beberg at –600 m /Munier et al. 1997/.*

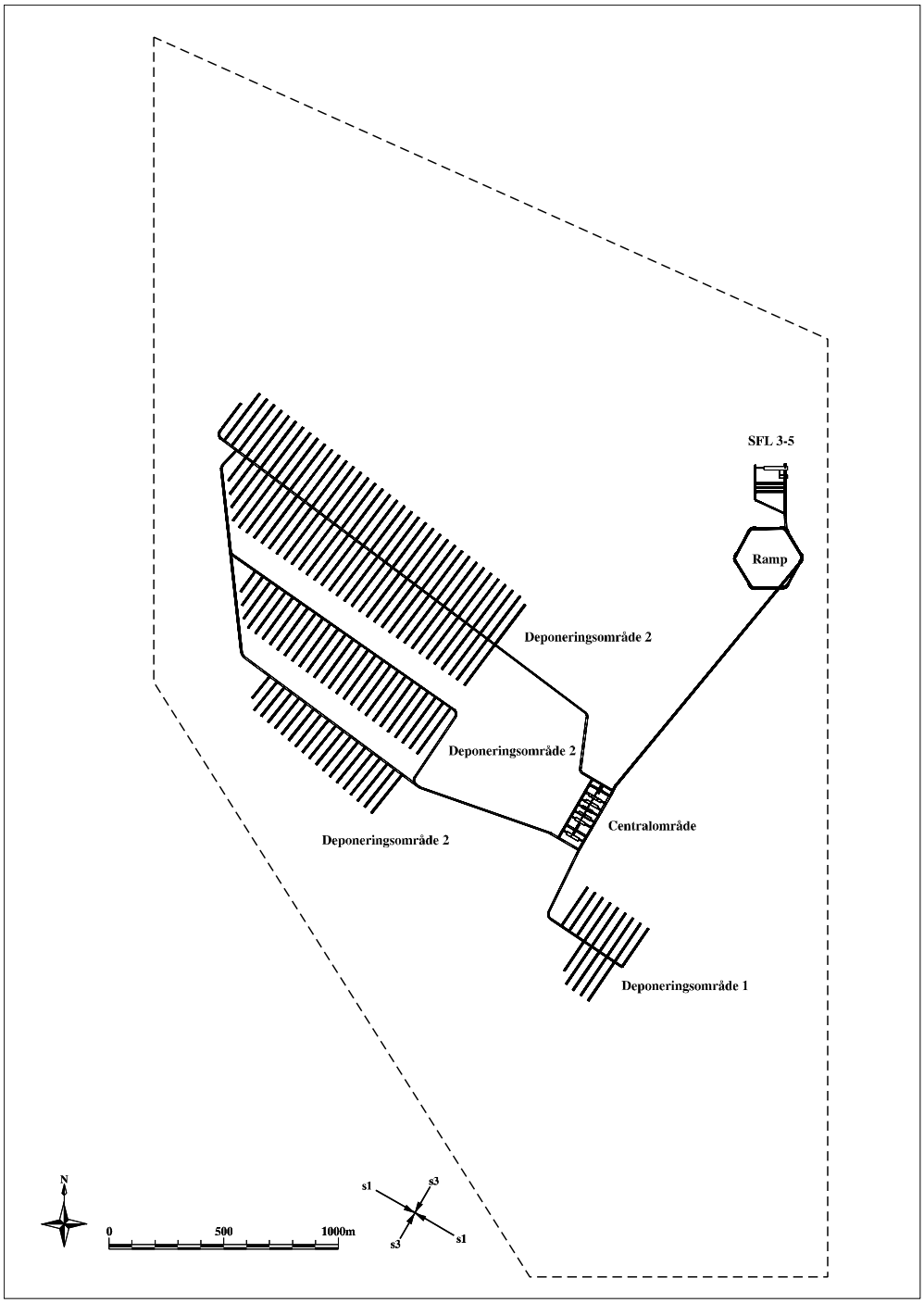

Figure A-2. *Layout of repository tunnels and roadways for Beberg at –600 m /Munier et al. 1997/.*

A screen-save from a session during the development of a FEMGV mesh for Task 3 is shown in Figure A-3.

Figure A-4 shows the position of the Task 3 canister-scale model in the context of the structural model at Beberg. It shows that Zone 10W cuts right through this tunnel system. In SR 97 Zone 10W was omitted for many reasons. One reason is that the conductivity for Zone 10W lower than the rock mass in SRD North. Another reason is that data for Zone 10 is based on a single borehole and the measurement is shallow depth (–14 masl). Saksa and Nummela question this zone as it is thin, 5 m, and has low conductivity. Also it may be seen in Figure A-2 that /Munier et al. 1997/ has omitted Zone 10W in designing the repository layout.

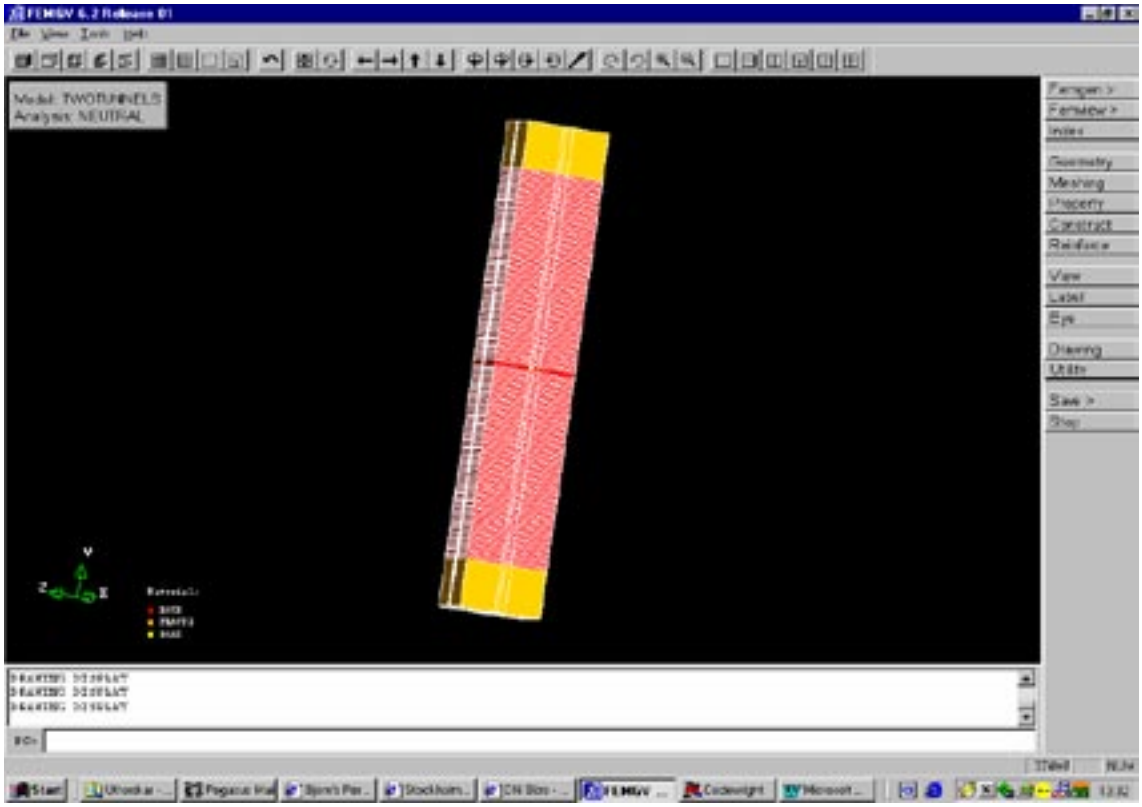

Figure A-3. *Construction of the mesh in FEMGV.*

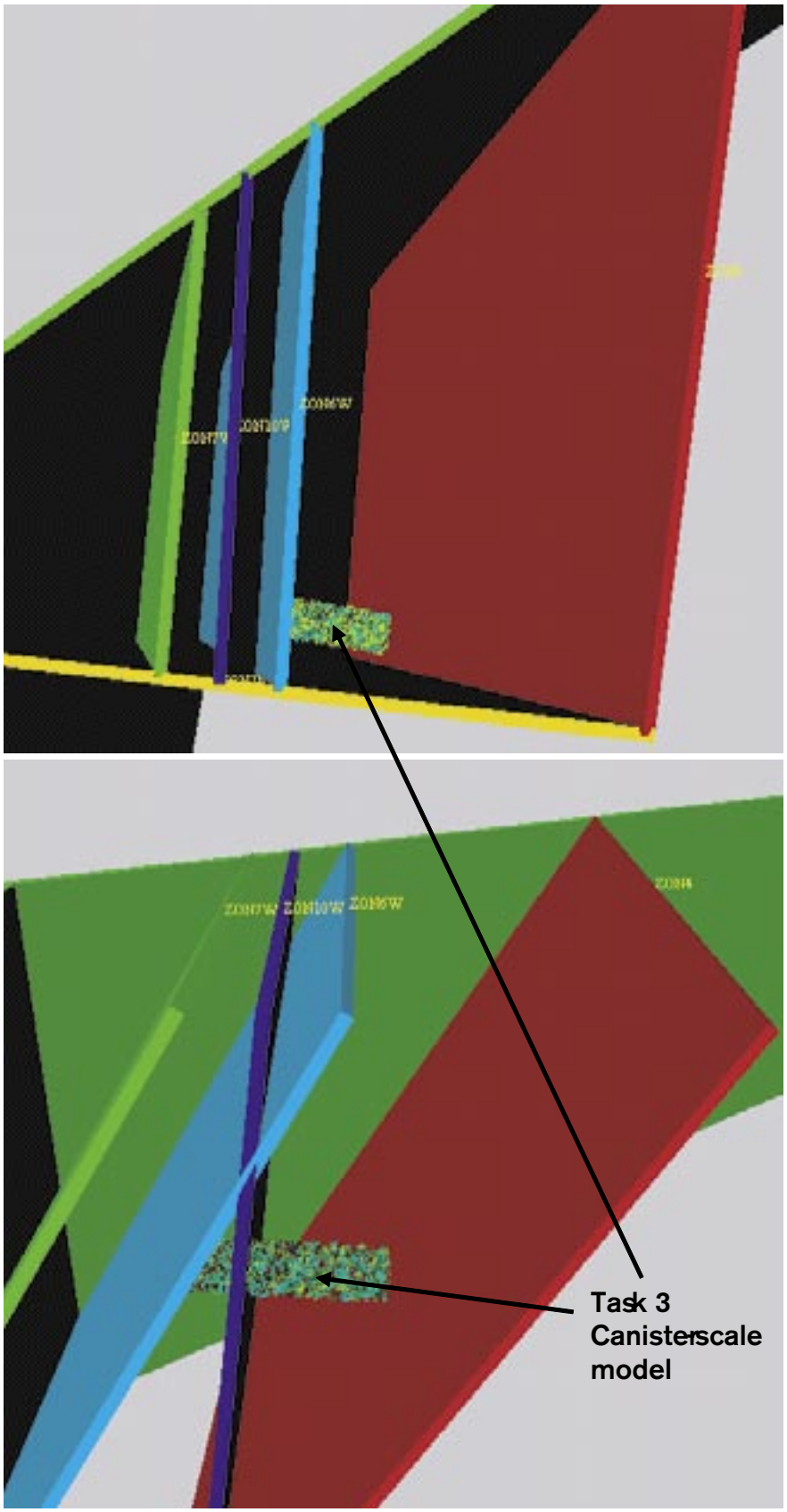

Figure A-4. *The position of the canister-scale model in the structural model of Beberg. Top: plan view of model with Zones 1, 4, 6, 7, 10 and 12. Bottom: view from the east with Zone 1 removed.*